Science Advances
AAAS

Supplementary Materials for

Genomic transformation and social organization during the Copper Age–Bronze Age transition in southern Iberia

Vanessa Villalba-Mouco*, Camila Oliart, Cristina Rihuete-Herrada, Ainash Childebayeva, Adam B. Rohrlach, María Inés Fregeiro, Eva Celdrán Beltrán, Carlos Velasco-Felipe, Franziska Aron, Marie Himmel, Caecilia Freund, Kurt W. Alt, Domingo C. Salazar-García, Gabriel García Atiénzar, Mª. Paz de Miguel Ibáñez, Mauro S. Hernández Pérez, Virginia Barciela, Alejandro Romero, Juana Ponce, Andrés Martínez, Joaquín Lomba, Jorge Soler, Ana Pujante Martínez, Azucena Avilés Fernández, María Haber-Uriarte, Consuelo Roca de Togores Muñoz, Iñigo Olalde, Carles Lalueza-Fox, David Reich, Johannes Krause, Leonardo García Sanjuán, Vicente Lull, Rafael Micó, Roberto Risch*, Wolfgang Haak*

*Corresponding author. Email: villalba@shh.mpg.de (V.V.-M.); robert.risch@uab.cat (R.R.); haak@shh.mpg.de (W.H.)

Published 17 November 2021, *Sci. Adv.* **7**, eabi7038 (2021)
DOI: 10.1126/sciadv.abi7038

The PDF file includes:

Other Supplementary Material for this manuscript includes the following:

Supplementary Text

1. Site descriptions and relevant archaeological information about sites and individuals successfully analyzed (following alphabetical order)

All prehistoric human skeletal remains for this study were collected with permission of the respective archaeological or state heritage organizations. All sample providers and collaboration partners are also co-authors and contacts persons for each site are given below.

● La Almoloya

Contact: *Vicente Lull, Cristina Rihuete Herrada, Rafael Micó, Roberto Risch, Eva Celdrán Beltrán, María Inés Fregeiro Morador, Camila Oliart Caravatti, Carlos Velasco Felipe*

La Almoloya (Pliego, Murcia) is a *ca.* 3,100 m^2 large El Argar settlement located in the northern foothills of Sierra Espuña. It is placed on a plateau 585 m a.s.l., *ca.* 35 km NE of La Bastida urban settlement. It was excavated by the UAB between 2013 and 2015 and is presently under restoration (*94*). According to the available 14C dates it was continuously occupied between 2200 and 1550 cal BCE, spanning the entire El Argar period. As in other El Argar sites, the architectural and stratigraphic sequence allows to differentiate three settlement phases, which can further be subdivided into subphases. During the early and middle phases, it seems to have been an important frontier settlement from where the El Argar expansion towards the North might have been organized, as the high proportion of warrior graves containing halberds suggests. During the final phase (1750-1550 cal BCE), La Almoloya not only developed an urban layout but also seems to have become a palatial center of the El Argar dominant class. One of its architectural complexes covered an area of 266 m^2 and was formed by six rooms with different economic and political functions. The largest one had continuous benches along all four walls and seems to have functioned as a space of political gathering. Under one of the benches, one of the richest tombs (AY-38) of EBA Europe was discovered (*95*). The genetic data of the couple buried in a large pottery vessel together with exceptional grave goods, as well as of other burials of the middle and late phases are included in the present study.

- ALM001 (Arc. ID: AY060/1): Adult female burial directly dated to 1955 - 1771 cal BCE (3544 ± 27, MAMS-26640).
- ALM002 (Arc. ID: AY060/2): Adult male burial directly dated to 1938-1771 cal BC (3532 ± 24, MAMS-25589).
- ALM003 (Arc. ID: AY053): Adult female burial dated indirectly by the archaeological context to the 3rd phase of El Argar (1750-1550 cal BCE).
- ALM004 (Arc. ID: AY058): Adult female burial dated indirectly by the archaeological context to the 2nd phase of El Argar (2000-1750 cal BCE).
- ALM006 (Arc. ID: AY067): Adult male burial directly dated to 1906-1772 cal BCE (3520 ± 14; RICH-22901/22907).
- ALM007 (Arc. ID: AY068/1): Adult male burial dated indirectly by the archaeological context to the 2nd phase of El Argar (2000-1750 cal BCE).
- ALM008 (Arc. ID: AY068/2): Adult female burial dated indirectly by the archaeological context to the 2nd phase of El Argar (2000-1750 cal BCE).

- ALM014 (Arc. ID: AY075): Infantile male burial dated indirectly by the archaeological context to the 2nd phase of El Argar (2000-1750 cal BCE).
- ALM015 (Arc. ID: AY080/1): Adult female burial directly dated to 1876-1751 cal BCE (3507 ± 24, MAMS-29729).
- ALM016 (Arc. ID: AY080/2): Adult male burial directly dated to 1841-1772 cal BCE (3534 ± 24, MAMS-29730).
- ALM017 (Arc. ID: AY080/0): Adult male in a secondary deposition directly dated to 1882-1700 cal BCE (3474 ± 25, MAMS-29728).
- ALM018 (Arc. ID: AY082/1): Adult female burial dated indirectly by the archaeological context to the 2nd phase of El Argar (2000-1750 cal BCE).
- ALM019 (Arc. ID: AY087): Adult female burial directly dated to 2120-1920 cal BCE (3631 ± 24, MAMS-32645).
- ALM020 (Arc. ID: AY090/1): Adult male burial dated indirectly by the archaeological context to the 2nd phase of El Argar (2000-1750 cal BCE).
- ALM021 (Arc. ID: AY090/2): Adult female burial dated indirectly by the archaeological context to the 2nd phase of El Argar (2000-1750 cal BCE).
- ALM024 (Arc. ID: AY094/1): Adult female burial dated indirectly by the archaeological context to the 2nd phase of El Argar (2000-1750 cal BCE).
- ALM025 (Arc. ID: AY094/2): Adult male burial dated indirectly by the archaeological context to the 2nd phase of El Argar (2000-1750 cal BCE).
- ALM026 (Arc. ID: AY096): Adult female burial dated indirectly by the archaeological context to the 2nd phase of El Argar (2000-1750 cal BCE).
- ALM027 (Arc. ID: AY097/1): Adult female burial dated indirectly by the archaeological context to the 2nd phase of El Argar (2000-1750 cal BCE).
- ALM028 (Arc. ID: AY097/2): Adult male burial dated indirectly by the archaeological context to the 2nd phase of El Argar (2000-1750 cal BCE).
- ALM029 (Arc. ID: AY104): Adult female burial dated indirectly by the archaeological context to the 3rd phase of El Argar (1750-1550 cal BCE).
- ALM030 (Arc. ID: AY030/1): Infantile female burial dated indirectly by the archaeological context to the 3rd phase of El Argar (1750-1550 cal BCE). Individual excluded from population genomic analysis due to 1st degree kin-relationship.
- ALM031 (Arc. ID: AY030/2): Infantile female burial dated indirectly by the archaeological context to the 3rd phase of El Argar (1750-1550 cal BCE). Individual excluded from population genomic analysis due to 1st degree kin-relationship.
- ALM032 (Arc. ID: AY005): Adult male burial dated indirectly by the archaeological context to the 3rd phase of El Argar (1750-1550 cal BCE).
- ALM033 (Arc. ID: AY012): Adult male burial directly dated to 1749 - 1659 cal BCE (3406 ± 16, MAMS-20878). Individual excluded from population genomic analysis due to <40000 SNP coverage.
- ALM034 (Arc. ID: AY016): Adult male burial directly dated to 1951-1774 cal BCE (3544 ± 24, MAMS-32644). Individual excluded from population genomic analysis due to 1st degree kin-relationship.
- ALM035 (Arc. ID: AY024/2): Adult female burial dated indirectly by the archaeological context to the 2nd phase of El Argar (2000-1750 cal BCE).

- ALM036 (Arc. ID: AY032): Adult male burial dated indirectly by the archaeological context to the 3rd phase of El Argar (1750-1550 cal BCE).
- ALM037 (Arc. ID: AY034): Adult female burial directly dated to 2016-1781 cal BCE (3567 ± 27, MAMS-25794). Individual excluded from population genomic analysis due to <40000 SNP coverage.
- ALM038 (Arc. ID: AY038/1): Adult female burial directly dated to 1746-1559 cal BCE (3366 ± 32, MAMS-22230).
- ALM039 (Arc. ID: AY038/2): Adult male burial directly dated to 1740-1533 cal BCE (33354 ± 33, MAMS-22231).
- ALM040 (Arc. ID: AY045): Adult male burial directly dated to 2008-1776 cal BCE (3555 ± 26, MAMS-25797).
- ALM041 (Arc. ID: AY046): Infantile male burial directly dated to 1941-1776 cal BCE (3540 ± 19, MAMS-39805).
- ALM042 (Arc. ID: AY047): Adult female burial dated indirectly by the archaeological context to the 2nd phase of El Argar (2000-1750 cal BCE).
- ALM043 (Arc. ID: AY048): Adult female burial directly dated to 1883-1701 cal BCE (3477 ± 24, MAMS-27900).
- ALM044 (Arc. ID: AY081): Adult female burial directly dated to 1897-1762 cal BCE (3512 ± 19, MAMS-39806).
- ALM045 (Arc. ID: AY082/2): Adult female burial dated indirectly by the archaeological context to the 2nd phase of El Argar. Individual excluded from population genomic analysis due to <40000 SNP coverage.
- ALM046 (Arc. ID: AY013): Infantile male burial directly dated to 1882-1751 cal BCE (3489 ± 20, MAMS-39801).
- ALM047 (Arc. ID: AY014): Infantile male burial dated indirectly by the archaeological context to the 2nd phase of El Argar (2000-1750 cal BCE).
- ALM048 (Arc. ID: AY022/1): Adult female burial dated indirectly by the archaeological context to the 2nd phase of El Argar (2000-1750 cal BCE).
- ALM049 (Arc. ID: AY022/2): Adult male burial dated indirectly by the archaeological context to the 2nd phase of El Argar (2000-1750 cal BCE).
- ALM050 (Arc. ID: AY024/1): Adult male burial dated indirectly by the archaeological context to the 2nd phase of El Argar (2000-1750 cal BCE).
- ALM051 (Arc. ID: AY037): Adult female burial dated indirectly by the archaeological context to the 3rd phase of El Argar (1750-1550 cal BCE).
- ALM052 (Arc. ID: AY042/1): Adult male burial directly dated to 1884-1754 cal BCE (3494 ± 19, MAMS-39803). Individual excluded from population genomic analysis due to 1st degree kin-relationship.
- ALM053 (Arc. ID: AY042/2): Adult female burial dated indirectly by the archaeological context to the 2nd phase of El Argar (2000-1750 cal BCE).
- ALM054 (Arc. ID: AY043). Adult female burial directly dated to 1884-1752 cal BCE (3492 ± 20, MAMS-39804). Individual excluded from population genomic analysis due to <40000 SNP coverage.
- ALM055 (Arc. ID: AY086): Adult female burial dated indirectly by the archaeological context to the 3rd phase of El Argar (1750-1550 cal BCE).
- ALM056 (Arc. ID: AY099): Adult female burial dated indirectly by the archaeological context to the 2nd phase (2000-1750 cal BCE).

- ALM057 (Arc. ID: AY025): Adult male burial directly dated to 1871-1686 cal BCE (3436 ± 19, MAMS-39802).
- ALM058 (Arc. ID: AY027/1): Adult male burial dated indirectly by the archaeological context to the 3rd phase of El Argar (1750-1550 cal BCE).
- ALM060 (Arc. ID: AY028): Infantile female burial directly dated to 1877-1687 cal BCE (3444 ± 23, MAMS-27899). Individual excluded from population genomic analysis due to 1st degree kin-relationship.
- ALM062 (Arc. ID: AY021/2): Neonatal female burial dated indirectly by the archaeological context to the 2nd phase of El Argar (2000-1750 cal BCE).
- ALM063 (Arc. ID: AY102): Infantile male burial dated indirectly by the archaeological context to the 3rd phase of El Argar (1750-1550 cal BCE).
- ALM064 (Arc. ID: AY050): Adult male burial dated indirectly by the archaeological context to the 3rd phase of El Argar (1750-1550 cal BCE).
- ALM067 (Arc. ID: AY073): Infantile female burial dated indirectly by the archaeological context to the 3rd phase of El Argar (1750-1550 cal BCE).
- ALM068 (Arc. ID: AY008): Infantile female burial dated indirectly by the archaeological context to the 3rd phase of El Argar (1750-1550 cal BCE).
- ALM069 (Arc. ID: AY095): Infantile male burial dated indirectly by the archaeological context to the 2nd phase of El Argar (2000-1750 cal BCE).
- ALM070 (Arc. ID: AY020): Infantile male burial dated indirectly by the archaeological context to the 3rd phase of El Argar (1750-1550 cal BCE).
- ALM071 (Arc. ID: AY093): Adult female burial dated indirectly by the archaeological context to the 3rd phase of El Argar (1750-1550 cal BCE).
- ALM073 (Arc. ID: AY021/1): Adult female burial directly dated to 1889-1765 cal BCE (3504 ± 16; MAMS-20881).
- ALM075 (Arc. ID: AY057): Infantile female burial dated indirectly by the archaeological context to the 2nd phase of El Argar (2000-1750 cal BCE).
- ALM076 (Arc. ID: AY077): Adult female burial dated indirectly by the archaeological context to the 3rd phase of El Argar (1750-1550 cal BCE).
- ALM077 (Arc. ID: AY017): Adult female burial dated indirectly by the archaeological context to the 3rd phase of El Argar (1750-1550 cal BCE).
- ALM078 (Arc. ID: AY023): Infantile male burial dated indirectly by the archaeological context to the 3rd phase of El Argar (1750-1550 cal BCE).
- ALM079 (Arc. ID: AY085/2): Neonatal female burial dated indirectly by the archaeological context to the 3rd phase of El Argar (1750-1550 cal BCE).
- ALM080 (Arc. ID: AY088): Infantile male burial dated indirectly by the archaeological context to the 3rd phase of El Argar (1750-1550 cal BCE). Individual excluded from population genomic analysis due to 1stdegree kin-relationship.
- ALM081 (Arc. ID: AY089): Infantile male burial dated indirectly by the archaeological context to the 3rd phase of El Argar (1750-1550 cal BCE).
- ALM084 (Arc. ID: AY105): Adult female burial dated indirectly by the archaeological context to the 3rd phase of El Argar (1750-1550 cal BCE).
- ALM086 (Arc. ID: AY026/2): Adult female burial directly dated to 1921-1771 cal BCE (3524 ± 21, MAMS-47169).

- ALM087 (Arc. ID: AY054): Adult female burial dated indirectly by the archaeological context to the 3rd phase of El Argar (1750-1550 cal BCE).
- ALM088 (Arc. ID: AY029): Adult female burial dated indirectly by the archaeological context to the 2nd phase of El Argar (2000-1750 cal BCE).

- **La Bastida**

Contact: *Vicente Lull, Cristina Rihuete Herrada, Rafael Micó, Roberto Risch, Eva Celdrán Beltrán, María Inés Fregeiro Morador, Camila Oliart Caravatti, Carlos Velasco Felipe*

La Bastida (Totana, Murcia) is a hilltop settlement that was naturally protected by vertical slopes and a monumental fortification, in a mountainous topography of the core area of El Argar formation. With an extension of *ca.* 4,5 ha it is one of the largest known EBA settlements of the Iberian Peninsula. An ample series of ^{14}C dates on short-lived material from funerary and domestic contexts has confirmed that the Argaric occupation lasted between ~2200 and 1600/1550 BCE, whereas the majority of the funerary structures can be dated after 1950 BCE. On the basis of stratigraphic and architectural reasons it is possible to distinguish an early (phase 1), a middle (phase 2), and a late phase (phase 3), dated respectively between ~2200-2000, ~2000-1750 BCE and ~1750-1600/1550 BCE. During the last two phases, the settlement developed into an urban center with large public constructions, such as water reservoirs (cisterns), and a clear division of tasks between buildings concentrating exceptional productive forces. The mineral, animal and botanic resources processed and used in La Bastida suggest that this urban center controlled a substantial territory, including the lower part of the fertile valley of the river Guadalentín. The distribution of these resources inside the settlement, its architecture, as well as the marked differences in wealth represented by the funerary assemblages, including individuals of both sexes and all ages, defines a class society with a politically and economically dominant elite (*32*, *96*, *97*).

- BAS002 (Arc. ID: BA06/1): Adult male burial directly dated to 1632-1506 cal BCE (3298 ± 27, KIA-50633).
- BAS003 (Arc. ID: BA12/2): Adult female burial directly dated to 2023-1913 cal BCE (3298 ± 27, KIA-50633).
- BAS006 (Arc. ID: BA18/1): Adult male burial dated indirectly by the archaeological context to the 3rd phase of El Argar. Individual excluded from population genomic analysis due to >40000 SNP coverage.
- BAS007 (Arc. ID: BA18/2): Adult male burial directly dated to 2018-1819 cal BCE (3568 ± 28, KIA-40012). Individual excluded from population genomic analysis due to >40000 SNP coverage.
- BAS014 (Arc. ID: Bamam 1): Individual excluded from population genomic analysis due to >40000 SNP coverage.
- BAS017 (Arc. ID: BA23/1): Infantile female burial directly dated to 1862-1687 cal BCE (3431 ± 15, KIA-40014/MAMS-10997). Individual excluded from population genomic analysis due to 1st degree kin-relationship.
- BAS018 (Arc. ID: BA23/2): Infantile male burial directly dated to 1750-1688 cal BCE (3423 ± 10, KIA-40015).
- BAS022 (Arc. ID: BA86): Adult male burial dated indirectly by the archaeological context to the 2nd phase of El Argar (2000-1750 cal BCE).

- BAS023 (Arc. ID: BA88): Adult male burial directly dated to 2122-2093 cal BCE (3642 ± 20, MAMS-19929).
- BAS024 (Arc. ID: BAH77-112.1): Adult male in secondary deposition directly dated to 2187-1981 cal BCE (3688 ± 23, MAMS-23111).
- BAS025 (Arc. ID: BA76): Infantile male burial directly dated to 2132-1949 cal BCE (3653 ± 21, MAMS-47168).
- BAS026 (Arc. ID: BA06/2): Neonatal male burial dated indirectly by the archaeological context to the 3rd phase of El Argar (1750-1550 cal BCE).
- BAS027 (Arc. ID: BA77): Adult female burial dated indirectly by the archaeological context to the 2nd phase of El Argar (2000-1750 cal BCE).

- **Cabezo Redondo**

Contact: *Gabriel García Atiénzar, Mª. Paz de Miguel, Mauro S. Hernández, Alejandro Romero, V. Barciela, Domingo C. Salazar-García*

This site is described in (7). We successfully analyzed one individual from this site:

- CBR001 (Arc. ID: Departamento XVIII/XX, CR89 Calle): Juvenile female burial directly dated to 1690-1535 cal BCE (3342 ± 21, MAMS-30748). Individual excluded from population genomic analysis due to <40000 SNP coverage.
- CBR004 (Arc. ID: CR03 Corte 2 UE03205/ Departamento 25): Infantile female burial directly dated to 1608-1450 cal BCE (3244 ± 20, MAMS-30750).

- **Camino del Molino**

Contact: *Joaquín Lomba Maurandi, Azucena Avilés Fernández, María Haber-Uriarte*

This site is described in (*98*). Camino del Molino is an accumulative mass grave located in a collapsed shelter. Analyzed individuals were taken only from the post-collapse stratigraphic unit, sealed by a boulder which avoided the percolation of materials from the previous phase. We successfully analyzed 5 new individuals from this site and we increased the coverage of one individual published in (*6*). The two previously published individuals are co-analyzed in this study.

- CDM001 (Arc. ID: CMOL 6): individual directly dated to 2550 - 2234 cal BCE (3910 ± 40, Beta-261517) coming from the post-collapse stratigraphic unit.
- CDM002 (Arc. ID: Individuo 12): Adult male individual directly dated to 2579 – 2346 cal BCE (3970 ± 40, Beta-261519)
- CDM003 (Arc. ID: CMOL 16): individual coming from the post-collapse stratigraphic unit.
- CDM004 (Arc. ID: CMOL 44): individual coming from the post-collapse stratigraphic unit.
- CDM005 (Arc. ID: CMOL 71): individual coming from the post-collapse stratigraphic unit.
- CDM006 (Arc. ID: CMOL 79): individual coming from the post-collapse stratigraphic unit.

- **Cova d'En Pardo (Planes, Alicante, Spain)**

Contact: *Jorge Soler, Consuelo Roca de Togores Muñoz, Domingo C. Salazar-García*

This site is described in (*98*). Excavations started in 1965 under Miquel Tarradell and continued from 1993 to 2007 by the MARQ of Alicante with a multidisciplinary approach. The actions overall reveal a deep stratigraphic sequence covering the periods from the Upper Palaeolithic to the Bronze Age. Levels III and IIb are related to a Late Neolithic funerary site. The deposit from these areas contained human remains pertaining to thirty individuals dating from ~3850-2850 cal BC, based on 7 absolute dates (*98*, *99*). No complete skeletons have been found. It is believed that human remains, once disarticulated, were placed against the walls and the bottom of the cavity, conforming an ossuary. While no metal objects have been found, among the funerary offerings we find an interesting set of adornments and costume elements in bone, as well as pottery with no decoration and a lithic industry with very elaborate arrowheads (*100*, *101*). We successfully analyzed 8 individuals from this site, all of which belong to skulls from the old excavations, which are deposited in the Museu Arqueològic Municipal Camil Visedo Moltó (Alcoi, Alacant):

- CDP001 (Arc. ID: 9090): Young adult female purportedly dating to the Late Neolithic/Copper Age
- CDP002 (Arc. ID: 9087): 20–25-year-old male purportedly dating to the Late Neolithic/Copper Age
- CDP003 (Arc. ID: 9085): 35–40-year-old male purportedly dating to the Late Neolithic/Copper Age. Individual excluded from population genomic analysis due to 1st degree kin-relationship.
- CDP006 (Arc. ID: 9084): 20–25-year-old male purportedly dating to the Late Neolithic/Copper Age
- CDP007 (Arc. ID: 9086): 17–20-year-old female purportedly dating to the Late Neolithic/Copper Age. Individual excluded from population genomic analysis due to >40000 SNP coverage.
- CDP008 (Arc. ID: 9109): Young adult of indeterminate sex purportedly dating to the Late Neolithic/Copper Age
- CDP009 (Arc. ID: 9101): Female adult purportedly dating to the Late Neolithic/Copper Age. Individual excluded from population genomic analysis due to 1st degree kin-relationship.
- CDP011 (Arc. ID: 9097): Female adult purportedly dating to the Late Neolithic/Copper Age

- **Cueva de las Lechuzas**

Contact: *Gabriel García Atiénzar, Alejandro Romero, Mª. Paz de Miguel Ibáñez, Domingo C. Salazar-García*

The cave is located on the eastern slope of the Cabezo de las Cuevas, a small hill in the centre of the Villena basin. The access and a part of the cave was destroyed by a quarry. Originally, the access was about 2 metres wide and gave way to the main room leaning towards the bottom.

When J.M. Soler visited the site, the owner of the quarry handed him a set of human bones that had appeared during the quarry work, later finding other human remains and various items of clothing. Soler identified human remains belonging to at least 18

individuals. He also recovered an important set of grave goods consisting of several arrowheads, an axe and a hoe on polished stone, several pendants on various species of seashell and on teeth and several necklace beads on fish and stone vertebrae. Several bone punches and several ceramic bowls were also documented. These trousseaus correspond to the use of the cavity during the Chalcolithic period. The type of collective burial in a cave with the associated grave goods indirectly date the collective necropolis to the Late Neolithic/Chalcolithic of Southeastern Iberia (3300-2300 cal BCE).

- CLL001 (Arc. ID: Lech 1(LE1)): Adult male burial dated indirectly to the Copper Age (3300-2300 cal BCE) by archaeological context.
- CLL002 (Arc. ID: Lech 2(LE2)): Adult female burial dated indirectly to the Copper Age (3300-2300 cal BCE) by archaeological context.
- CLL003 (Arc. ID: Lech 3(LE3)): Adult male burial dated indirectly to the Copper Age (3300-2300 cal BCE) by archaeological context.
- CLL004 (Arc. ID: Lech 5 (LE5)): Adult male burial dated indirectly in Copper Age (3300-2300 cal BCE) by archaeological context.
- CLL005 (Arc. ID: Lech 7 (LE7))*: Adult male burial dated indirectly to the Copper Age (3300-2300 cal BCE) by archaeological context.
- CLL006 (Arc. ID: Lech 8 (LE8): Adult female burial dated indirectly to the Copper Age (3300-2300 cal BCE) by archaeological context.
- CLL007 (Arc. ID: Lech 11 (LE11B)): Adult male burial. This individual was considered intrusive and thus excluded from the analysis, as it showed steppe-related ancestry. The remainder of the individuals are genetically similar to the SE_Iberia_CA group, so we assumed the indirect chronology for all of them.
- CLL008 (Arc. ID: Lech 11bis (inf) (LE11A)): Infantile male burial dated indirectly to the Copper Age (3300-2300 cal BCE) by archaeological context.
- CLL009 (Arc. ID: Lech 14-6 (LE6)): Adult male burial dated indirectly to the Copper Age (3300-2300 cal BCE) by archaeological context.
- CLL010 (Arc. ID: Lech 14bis (LE14)): Juvenile female burial dated indirectly to the Copper Age (3300-2300 cal BCE) by archaeological context.
- CLL011 (Arc. ID: Lech X3): Adult male burial dated indirectly to the Copper Age (3300-2300 cal BCE) by archaeological context.

- **Cerro del Morrón**

Contact: *Vicente Lull, Cristina Rihuete Herrada, Rafael Micó, Roberto Risch, Eva Celdrán Beltrán, María Inés Fregeiro Morador, Camila Oliart Caravatti, Carlos Velasco Felipe*

Cerro del Morrón (Moratalla, Murcia) is a small hilltop settlement located 1065 m a.s.l. in the Eastern part of the Betic mountain range. A rescue excavation carried out in 2016 allowed to recover the human remains of two already robbed burials and to investigate the stratigraphic sequence of the site. The first settlement, dated ca. 2050-1950 cal BCE, did not include characteristic materials of El Argar but shows clear affinities with the EBA of the southern part of the *Meseta* (central Spanish plateau). At a certain moment the site became part of the northern borders of the El Argar territory. The two ditch burials with stone lining contained double inhumations and belong to this 2nd, highly

eroded phase. According to the absolute dating of the two inhumations from one of the burials the settlement was occupied between ~1800-1750 cal BCE.

- CMO001 (Arc. ID: MN-1/1): Adult female burial directly dated to 1879-1691 cal BCE (3455 ± 28, MAMS-11823).
- CMO002 (Arc. ID: MN-1/2): Adult male burial directly dated to 1887-1747 cal BCE (3492 ± 24, MAMS-11824).
- CMO003 (Arc. ID: MN-2/1): Adult female burial.

- **Es Forat de ses Aritges**

Contact: *Vicente Lull, Rafael Micó, Cristina Rihuete Herrada, Roberto Risch*

This site is described in (*98*). This Late Bronze Age stratified collective funerary cave with a megalithic entrance was excavated in 1995. Nine randomly sampled individuals, buried in different layers, have been dated (*102*). According to these results the funerary structure was used between c. 1400-1000/800 cal BCE (*102*, *103*).We successfully analyzed 6 individuals from this site:

- EFA001 (Arc. ID: FA32-3592): Adult male from a collective burial indirectly dated to the Late Bronze Age (1200-1000 cal BCE). Individual excluded from population genomic analysis due to <40000 SNP coverage.
- EFA004 (Arch. ID: FA49-9819): Adult female from a collective burial indirectly dated to the Late Bronze Age (1200-1000 cal BCE). Individual excluded from population genomic analysis due to <40000 SNP coverage.
- EFA006 (Arc. ID: FA11-8250): Adult male from a collective burial indirectly dated to the Late Bronze Age (1200-1000 cal BCE).
- EFA007 (Arc. ID: FA39-10299): Adult male from a collective burial indirectly dated to the Late Bronze Age (1200-1000 cal BCE). Individual excluded from population genomic analysis due to 1st degree kin-relationship.
- EFA008 (Arc. ID: FA24-3307): Juvenile male from a collective burial indirectly dated to the Late Bronze Age (1200-1000 cal BCE).
- EFA009 (Arc. ID: FA36B-5058): Adult male from a collective burial indirectly dated to the Late Bronze Age (1200-1000 cal BCE).
- EFA010 (Arc. ID: FA32-3578): Adult female from a collective burial indirectly dated to the Late Bronze Age (1200-1000 cal BCE).
- EFA011 (Arc. ID: FA7-1961): Adult female from a collective burial indirectly dated to the Late Bronze Age (1200-1000 cal BCE).

- **Fuente Álamo**

Contact: *Roberto Risch*

This site is described in (*98*). We analyzed 6 individuals from this site:

- FAL001 (Arc. ID: 75). Adult female individual directly dated to 2116-1693 cal BCE (3545 ± 65, OxA-4972). Individual excluded from population genomic analysis due to <40000 SNP coverage.
- FAL002 (Arc. ID: 75a). Adult male individual directly dated to 2141-1885 cal BCE (3635 ± 50, OxA-4973). Individual excluded from population genomic analysis due to <40000 SNP coverage.
- FAL007 (Arc. ID: 69). Adult individual dated indirectly by the archaeological context to the 2nd phase of El Argar (2000-1750 cal BCE).

Individual excluded from population genomic analysis due to <40000 SNP coverage.

- **La Horna**

Contact: *Gabriel García Atiénzar, Mª. Paz de Miguel, Mauro S. Hernández, Alejandro Romero, Domingo C. Salazar-García*

The site occupies the summit and eastern slope of a hill in the northwestern foothills of the mountain range of the same name. The settlement stands about 75-100 metres above the flat areas of the Novelda basin, at about 439 m above sea level. Its maximum extension would be around 1000 m^2. The process of excavation (1980-1986) documented a unique Late Bronze Age phase that would be dated to the middle of the 2nd millennium BCE. The excavations made it possible to differentiate 8 rooms and a possible street. The rooms are small and irregular in plan, with paved surfaces and roofs supported by posts. In certain rooms the entire cereal harvest was managed and in others the production of instruments and objects necessary for the maintenance of the group was carried out. Two small crevices, used as funeral spaces, were also documented. In cave 1, inside the area of the settlement, several very altered human remains were recovered, most of them belonging to children - NMI: 8 - and a silver earring as a grave good. In cave 2, located on the hill but outside the settlement, a possible cist was identified that housed human remains - fragments of a femur, humerus, a rib, clavicle and several skull fragments.

- LHO001 (Arc. ID: Individuo 1): Infantile male burial directly dated to 1613 - 1451 cal BCE (3250 ± 30, Beta-397978).
- LHO002 (Arc. ID: Individuo 2): Infantile male burial directly dated to 1630 - 1497 cal BCE (3280 ± 30, Beta-397977). Individual excluded from population genomic analysis due to 1st degree kin-relationship.
- LHO003 (Arc. ID: Individuo 3): Infantile female burial directly dated to 1661 - 1509 cal BCE (3310 ± 30, Beta-397979).

- **Lorca**

Contact: *Andrés Martínez, Juana Ponce Martínez.*

This site, which includes the burials found during the rescue excavations of **Madres Mercedarias** church, **Castillo de Lorca** and **Los Tintes** and **Zapatería 11** streets, belongs to the core area of El Argar. All excavations have confirmed that the in-tramural burials belong to the El Argar phases. It is described in (*98*).

We successfully analysed 3 individuals from this site:

- CDL001 (Arc. ID: Castillo de Lorca Loct4): Adult female burial indirectly dated by the archaeological context to the middle or late El Argar phases (2000-1550 BCE). Individual excluded from population genomic analysis due to <40000 SNP coverage.
- LOT001 (Arc. ID: Los Tintes 2-1): Adult male burial directly dated to 2021-1773 cal BCE (3560 ± 35, OxA-7667).
- MMI002 (Arc. ID: Tomb 11-1): Adult female burial directly dated to 1940-1700 cal BCE (3510 ± 40, OxA-7672). Individual excluded from population genomic analysis due to <40000 SNP coverage.
- MMI003 (Arc. ID: Tomb 4-1): Adult female burial directly dated to 1879-1692 cal BCE (3456 ± 27, OxA-17056). Individual excluded from population genomic analysis due to <40000 SNP coverage.

- MMI004 (Arc. ID: Tomb 4-2): Adult male burial indirectly dated by the archaeological context to the 3rd phase of El Argar (1750-1550 cal BCE).
- ZAP001(Arc. ID: Urna 3 Tumba 3): Adult male burial indirectly dated by the archaeological context to the 3rd phase of El Argar (1750-1550 cal BCE). Individual excluded from population genomic analysis due to <40000 SNP coverage.
- ZAP002 (Arc. ID: Tumba 6): Adult male burial indirectly dated by the archaeological context to the 3rd phase of El Argar (1750-1550 cal BCE).

- **Molinos de Papel**

Contact: *Ana Pujante Martínez, María Inés Fregeiro Morador, Camila Oliart Caravatti, Cristina Rihuete Herrada*

This site is described in (*98*). We successfully analysed 3 individuals from this site:

- MDP001 (Ar. ID: MP1039): Adult male burial directly dated to 2296-2060 cal BCE (3780 ± 30, MAMS-11826). Individual excluded from population genomic analysis due to 1st degree kin-relationship.
- MDP002 (Ar. ID: MP1059): Adult female burial directly dated to 2200-2027 cal BCE (3711 ± 29, MAMS-11827).
- MDP003 (Ar. ID: MP1065): Adult male burial directly dated to 2196-2023 cal BCE (3701 ± 26, MAMS-11828).

- **Miquel Vives**

Contact: *Camila Oliart Caravatti*

This site is described in (*98*). We successfully analyzed one individual from this site:

- MIV002 (Arc. ID: Miquel Vives 259): Infantile female in a collective burial dated to 1690-1500 cal BCE (3310 ± 35, KIA-35362).

- **Valencina (PP4-Montelirio) (Castilleja de Guzmán, Sevilla)**

Contact: *Leonardo García Sanjuán*

A total of 42 samples of human bone were analysed from the PP4-Montelirio Sector and the Montelirio tholos, both belonging to the Copper Age Valencina de la Concepción-Castilleja de Guzmán (for short, Valencina) mega-site, occupied between c. 3200 and 2350 BCE. Sufficient amounts of authentic ancient human DNA could not be retrieved from 31 individuals (including all 12 from the Montelirio tholos) and only 11 yielded aDNA results, which are included here. Nine of the eleven successfully sequenced individuals come from Structure 10.028, a simple pit without stone elements dated to between 2900 and 2700 BCE (2890-2637 cal BC 2σ, 4180 ± 35 BP, CNA-4797), that yielded no grave goods:

- MON013 (Ar. ID: Individuo 1, Structure 10028 UE189): adult individual, anthropologically described as “possible female”.
- MON014 (Ar. ID: Individuo 2, Structure 10028 UE189): adult male individual.
- MON015 (Ar. ID: Individuo 3, Structure 10028 UE189): young adult individual, anthropologically described as “possible female”.
- MON016 (Ar. ID: Individuo 4, Structure 10028 UE189): adult individual, anthropologically described as “possible male”.

- MON017 (Ar. ID: Individuo 5, Structure 10028 UE189): adult male individual.
- MON019 (Ar. ID: Individuo 7, Structure 10028 UE189): young adult individual, anthropologically described as “possible male”.
- MON020 (Ar. ID: Individuo 8, Structure 10028 UE189): adult male individual.
- MON021 (Ar. ID: Individuo 9, Structure 10028 UE189): young adult individual, anthropologically described as “possible female”.
- MON029 (Ar. ID: Individuo 1, Structure 10031, UE453): adult male individual dated indirectly to the Copper Age (2800-2400 BCE) by archaeological context.
- MON033 (Ar. ID: Individuo 2, Structure 10073, UE866): adult individual, anthropologically described as “possible female”, indirectly to the Copper Age (3200-2350 BCE).
- MON036 (Ar. ID: Individuo 2, Structure 10044, UE632): adult male individual, indirectly to the Copper Age (3200-2350 BCE).

- **Peñón de la Zorra (eastern cave)**

Contact: *Gabriel García Atiénzar, Mª. Paz de Miguel Ibáñez, Alejandro Romero, Domingo C. Salazar-García*

Small cavity located in the oriental slope of the mountain range of the Morrón at about 640 m asl. Its entrance was covered by large limestone blocks at the time of its excavation, carried out by José María Soler in spring 1964. It is located on the same hill as the town of the same name, where several phases of occupation have been recognised between the Bell-Beaker (Phase 1: ca. 2400 cal BCE) and the Bronze Age (Phases 2-4: ca. 2100-1700 cal BCE). The human remains were completely removed. They correspond to at least six individuals, three adults and three children (4, 6-8 and 10-12 years), both sexes being represented. The adult individuals show high wear of their teeth, which can be related to age. Associated with these remains several copper weapons were recovered: a tongue dagger and a pair of Palmella-type points. A silver earring with a diameter of 1.3 cm, a necklace made up of 14 fish vertebrae and several small bowls were also recovered. All three adults have been dated from samples obtained from their left femora (MAMS-19108: 3357±22 BP; Poz-73601: 3330±35 BP; Poz-73603: 3405±35 BP). However, due to the state of preservation of the record, it is impossible to decide which individual corresponds to the pars petrosa analysed (PLZ001). In any case, the chronological proximity of the radiometric dates implies that PLZ001 can be dated reliably to 1750-1600 BCE. This time span is consistent with some of the documented artefacts such as silver earrings, necklace beads made from fish vertebrae as well as several small bowls.

- PLZ001(Arc. ID: Individuo 1): Adult female burial indirectly dated in Bronze Age (1750-1600 cal BCE) by archaeological context

- **Cueva del Puntal de los Carniceros**

Contact: *Gabriel García Atiénzar, Mª. Paz de Miguel Ibáñez, Alejandro Romero, Domingo C. Salazar-García*

Small cavity located on the western slope of the Sierra del Morrón, at about 620 m above sea level. On the same hill it is located a settlement in which Bell-Beaker levels have

been documented. In the excavation carried out in the cave in 1964 by J.M. Soler, a first layer of topsoil was documented, superimposed on a greyish package where human remains, and grave goods were found. The remains of at least seven individuals have been identified, five adults of both sexes, one juvenile between 12-15 years old and a child of about 2-4 years old. A case of dental loss has been identified, as well as evidence of mandibular osteoarthritis in one of the individuals. The graves goods are heterogeneous, highlighting some knapped stone tools -an arrowhead, a geometric microlite-, a silver earring, several necklace beads made from different raw materials and ceramic fragments corresponding to small bowls.

- PUC001 (Arc. ID: Cráneo 2): Adult female burial directly dated to 1879 - 1695 cal BCE (3461 ± 19, MAMS-24730).
- PUC002 (Arc. ID: Cráneo 3): Adult male burial directly dated to 1736 – 1622 cal BCE (3371 ± 19, MAMS-24725).
- PUC003 (Arc. ID: Cráneo 4): Adult female burial directly dated to 1882 - 1749 cal BCE (3486 ± 20, MAMS-24728).
- PUC004 (Arc. ID: Cráneo 5): Juvenile female burial directly dated to 1751 – 1643 cal BCE (3407 ± 19, MAMS-24729).

2. Mitochondrial haplogroup determination

We generated complete mitogenomes using an independent mt-capture (*4*, *40*) (**table S1.3**). In cases where the number of mt reads was below 3,000, we performed a 2nd round of capture. For some individuals we were able to determine the mt haplogroup although we did not obtain nuclear data in sufficient amounts. A summary of mtDNA results is given in **table S1.4**.
We determined seven different major haplogroups in our reported CA individuals. Most of them were already reported for Iberian Neolithic and CA. We found a new haplotype U5a1c1a, although U5a1c was already reported in Iberia CA (*104*).

We determined 18 different haplogroups in our new BA individuals. Most of them were already reported for Iberian Neolithic, CA and BA groups. We briefly described here the ones which have not been reported yet. We determined the haplogroups H105a and H10b (BAS025 and EFA008) not reported so far in Iberia. Haplogroup H10* has been previously reported in Germany Bell Beaker (H10e) (*6*), Croatia_Sopot_MN (H10) (*76*), Kazakhstan_centralSaka.SG (H10 and H101) (*105*) and Latvia_BA (H10a) (*106*). We determined the haplogroup H1bd in ALM029. Haplogroups H1 have been reported in Iberia since the EN ((*24*), Pancorbo), MN and CA (Paris, Cmolino, (*6*)). Haplogroup H1cf has been determined in ALM064. The same haplogroup has been reported in today's Canary_Islands_Guanche, (*107*).

We determined the haplogroup H6a1b in ALM047. This haplogroup has been previously found in Yamnaya_Samara (*4*), Russia_Afanasievo (*108*), England_Bell_Beaker (*6*) and Russia_Okunevo_EMBA.SG (*105*). We determined the haplogroup I1a1 in PUC002. I1 has been previously reported for later Iron Age in Iberia (*7*). I1a1 has been reported in Russia Srubnaya (*22*), Croatia MBA (*76*) and Poland_Chopice_Vesele (*6*). K2a reported in ALM084 has been determined in later periods in Iberia (NE_Iberia_Greek from Empuries) (*7*), despite the haplogroup is usual among in Neolithic groups (Germany LBK, (*24*), Hungary_Vinca_MN (*24*), Hungary_Balaton_Lasinja_CA (*24*) and Mesolithic from Iran (Iran_Belt_Cave) (*108*).

Interestingly, we determined R0a in ALM018. R0 haplogroup (pre-HV) has not been reported from Iberia so far.Nowadays, this haplogroup is more frequent in the Arabian Peninsula, but has been found in ancient individuals from the eastern Mediterranean, e.g. Jordan_PPNB (R0a), Jordan_PPNC (R02a), Jordan_EBA (R0a1a) (*23*), as well as Ukraine_Yamnaya (R0a1) (*76*) and Sicily_Bell_Beaker (R0a) (*6*). The fact that R0a has not been found in central Europe despite hundreds of data points suggests that this haplogroup was rare or absent in this region, and suggests the Mediterranean region as a route of dissemination during the CA and EBA.

3. Y-chromosome haplogroup determination

We were able to confirm the almost-complete turnover in Y-chromosome lineages during the CA-EBA transition as described in (*7*), despite a tripling of the BA individuals analyzed to date. All pre-BA individuals belonged to the already described Y-haplogroups I2a, G2a and H2. I2a was attributed to hunter-gatherers and, G2a and H2 to early European farming groups. These haplogroups are absent in all EBA individuals analyzed so far, in favor of sub-lineages of R1b-M269 (**Table S1.1**). The exact phylogenetic position on the Y haplogroup tree could be resolved further in 41 out of 49 males, who carry the derived variant at Y-SNP P312, and Y-SNP Z195 in 23 out of 41 males. The low coverage genome of individual ALM041 resolves this Y lineage until Y-SNP S228. It is possible that all other males also belonged to the same or a closely related branch. Only one subadult male individual (BAS025) was assigned to E1b1b1a1b1. He was dated to the 2nd phase of El Argar (2000 - 1750 cal BCE), being one of the very few and late non-R1b-M269 males in the Iberian BA. Y-Haplogroup E1b1b1a was reported from Sardinia Chalcolithic, E1b1b1b2 in Early Medieval Sardinia (*51*), and E1b1b1a1b1 in Medieval Sardinia (*52*).

4. Chromosomal disorders

We used the fraction of reads mapping to the X and Y chromosome vs. the autosomes (X-ratio *vs.* Y-ratio) as implemented in ANGSD (*44*) to determine the genetic sex for each individual. We also found two individuals with chromosomal disorders, which we briefly describe here:

4.1 XXY aneuploidy (Klinefelter syndrome) in individual CLL011

The Syndrome originally described in (*109*) consisted of gynecomastia and aspermatogenesis. It was previously thought to be a hormonal disorder until (*110*) defined the syndrome as chromosomal disorder caused by an extra X chromosome in genetically male individuals (47, XXY). The symptoms and traits are tall stature, hypogonadism, fertility problems and sometimes difficulties in learning. The prevalence is 1 in 650 male births (*111*).
The individual CLL011 shows an X-ratio (see **Materials and Methods***,* **table S1.1**) of 0.80, similar to genetically female individuals, but a Y-ratio of 0.46, similar to genetically male individuals, which is indicative of an XXY karyotype. Levels of mtDNA contamination are low (0.36%) and render female contamination unlikely (**fig. S1, table S1.1**), while the commonly used ANGSD method for male individuals is not applicable in this case. Individual CLL011 is reported anthropologically as an adult individual but no further morphological details were given. Other aDNA studies have also reported XXY cases recently (*58*, *112*).

4.2 Trisomy X (Triple-X syndrome) in individual ALM062

The trisomy X or triple-X syndrome was described (*110*) as chromosomal disorder caused by an extra/supernumerary X chromosome in genetically female individuals (47, XXX). Clinical symptoms are often absent or unnoted, and, if present, are variable and usually related to delayed speech development and psychiatric disorders, early growth with longer legs and sometimes infertility (*113*, *114*). The prevalence is approximately 1 in 1000 female births (*110*).

The neonatal individual ALM062 shows a Y-ratio of 0.01, as expected for genetically female individuals, but a X-ratio of 1.18, consistent with 1.5 higher than males and 0.5 times higher than females, and thus indicative of an XXX karyotype. Levels of mtDNA contamination are sufficiently low (0.4%) to exclude additional female contamination (**fig. S1, table S1.1**).

5. Kinship

We used three different methods to estimate the degree of kinship based on genome-wide from the newly typed individuals, including LcMLkin (*47*)(**fig. S2A** and **fig. S2B**), PWMR (*48*), **fig. S2C**) and READ (*49*), **table S1.5, table S1.6** and **table S1.7**) for pseudo-haploid data (see methods). We also confirmed the 1st or 2nd degree related pairs by way of *f3*-outgroup statistics of the form *f3(ind1, ind2; Mbuti)* (**fig. S2D**).

6. Population group labels

For the co-analyzed Middle Late Neolithic (MLN) and Copper Age (CA) Iberian individuals from previous publications, we kept the labels as used in (*7*), and followed the chronological and geographical naming scheme for our newly reported individuals, resulting in **SE/SW_Iberia_CA** (Southeast, Southwest) (**table S2.1**).

For the Bronze Age (BA) Iberian individuals, we used the same principle (*7*), resulting in **N/NE/C/SE/SW _Iberia_BA** (North, Northeast, Northwest, central, Southeast, Southwest). Concerning the group **SE_Iberia_BA**, we pooled individuals, who are assigned to the El Argar group as **SE_Iberia_BA_Argar** and those associated with the Valencian BA as **SE_Iberia_BA_Valencian**. In order to explore the groupings at higher resolution, we kept individuals from the site Molinos de Papel separated (**MolinosPapel_EBA)**, as it is one of the earliest sites that shows Argaric features in the archaeological record (e.g. intramural burials, double burials, presence of a silver ornament), but cannot be considered a typical El Argar hilltop settlement nor funerary context). We further grouped the few individuals from the extended territory of a late phase El Argar group (Cerro de la Virgen in Granada) as **CerroVirgen_Late_Argar**, already reported in (*7*). We also grouped the published (*7*) and newly reported individuals from the site Cabezo Redondo in Alicante separately as **SE_CabezoRedondo_BA,** as this site in the Valencian territory also shows Argaric features. The main El Argar sites, La Almoloya and La Bastida (**Bastida_Argar)**, were also analyzed separately, to allow for temporal grouping. Individuals from La Almoloya were further divided according to settlement phases as **Almoloya_Argar_Early** and **Almoloya_Late_Argar**.

Outlier individuals already reported in (*7*) were tagged with different labels (**C_Iberia_CA_Afr** from Camino de las Yeseras and **SW_Iberia_BA_Afr** from Loma del Puerco) and not included in any CA or BA groups. We also analyzed the new outlier individual from the site Zapatería (**ZAP002**) independently. For the remainder of the prehistoric European groups, we kept labels as used in the respective publications (**table S2.1**).

7. Ancestry modelling of Copper Age individuals

7.1 Connections between southern Iberia Copper Age and the Mediterranean

The location of southern Iberia MLN and CA groups in comparison with northern MLN and CA on the PCA plot suggests a small amount of HG ancestry, as it has been shown that a leftward shift along PC1 reflects an increasing amount of HG ancestry in later Neolithic groups (*4*, *24*). However, when we model this ancestry component with *qpAdm* **(fig. 2D**) we observe that the HG-related ancestry is not only quantitatively distinct from preceding Neolithic groups but also distinguishable qualitatively. We find that southern MLN and CA groups carry a subtle Magdalenian-like ancestry compared to northern Iberian ones (**fig. 2B, fig. 2C** and **fig. 2D**).

The *qpAdm* model used to produce **fig. 2D** (model 1) is part of a series of more extended models as detailed below:

7.1.1 Model 1a

Target: Iberian MLN and CA, eastern European CA, and CA and EBA central Mediterranean groups
Sources: Anatolia_N and WHG, Anatolia_N, WHG and GoyetQ2, or Anatolia_N, WHG and EHG (exploring 2 or 3-way admixture models)
Outgroups: Mbuti.DG, Ethiopia_4500BP.SG, Ust_Ishim.DG, Russia_MA1_HG.SG, Italy_Villabruna, Belgium_GoyetQ116_1_published, Han.DG, Onge.DG, Papuan.DG, AHG, CHG, Morocco_Iberomaurusian

Please see **tables S2.4** and **table S2.5** for detailed *qpWave* and *qpAdm* results.

This model was used to differentiate between northern and southern Iberian MLN and CA groups which formed subtle sub-groups in PC space. The model was also applied to eastern European CA and EBA central Mediterranean groups. Detailed results for Iberian CA and EBA groups are shown in **table S2.4** and for the rest of CA and EBA Europeans in **table S2.5.**

Including individual Belgium_GoyetQ116-1_published in the outgroups is essential to model the Magdalenian-associated ancestry represented by GoyetQ2, while AHG fulfills this purpose for the Anatolia_N component, and Italy_Villabruna for the WHG-related sources. Here, we only include individuals Loschbour and KO1 in WHGs, and exclude La Brana1 which was shown to carry a substantial proportion of GoyetQ2-like ancestry. We included EHG as a source that is interchangeable with GoyetQ2 to test whether the modelled HG ancestry proportion is specifically Magdalenian-related and unrelated to other potential HG ancestry sources such as EHG.
In Iberia, SE_Iberia_MLN, SW_Iberia_MLN and SW_Iberia_CA could not be modelled successfully as two-way admixture of Anatolia Neolithic and WHG (p-values below 0.05), but

the model found support when GoyetQ2 was added as a third source. For SE_Iberia_CA we note that the model fit could be improved from a p-value of 2.53E-06 to 0.008 (**table S2.4, fig. 2D**) by adding GoyetQ2. This suggests a subtle presence of Magdalenian ancestry, in line with the results from the *f4*-statistics (**fig. 2C**) and the geographical pattern described for the remainder of Iberian groups. When we exchanged GoyetQ2 by EHG, none of the models improved their fit (**table S2.4**). To confirm that the ancestry source that is needed in southern Iberians was related to GoyetQ2 and not to any other HG-ancestral source, we rotated GoyetQ2 to the outgroups and added EHG as a source. By doing so, all models for southern Iberian groups were rejected. In turn, when EHG was added to the outgroups p-values for southern Iberian groups remained >0.05. We thus showed that the three-way competing model and rotating strategy returned consistent results (**table S2.4)**.

In CA and EBA central Mediterranean and eastern European CA, we observed that adding either GoyetQ2 or EHG as third source does not improve any model compared to their respective two-way model with Anatolia_N and WHG. We conclude that the Magdalenian-associated component represented by GoyetQ2 was absent/not detectable in other Mediterranean and contemporaneous groups (**table S2.5**).

7.1.2 Model 1b

Target: Iberian MLN and CA, eastern European CA, and CA and EBA central Mediterranean groups
Sources: Anatolia_Neolithic, WHG and Iran_N/ Russia_Yamnaya_Samara/Jordan_PPNB
Outgroups: Mbuti.DG, Ethiopia_4500BP.SG, Ust_Ishim.DG, Russia_MA1_HG.SG, Italy_Villabruna, Belgium_GoyetQ116_1_published, Han.DG, Onge.DG, Papuan.DG, AHG, CHG, Morocco_Iberomaurusian.

Applying the two-way "Model 1a" (Anatolia_N plus WHG) resulted in a poor fit in many central Mediterranean target groups, which was interpreted as missing a third or more ancestry components. To test if adding a third source improved the model fit, we exchanged GoyetQ2 from "Model 1a" with either Iran_N or Yamnaya_Samara. The qpWave and *qpAdm*results for each combination of sources are reported in **table S2.4** and **table S2.5**.

We obtained a similar result when adding Yamnaya_Samara as a third source, which precludes the presence of steppe-related ancestry along the Central Mediterranean around this time, with the exception of Italy_Bell_Beaker. However, by adding Iran_N as a source most of the previously rejected models returned p-values of ≥0.05, e.g. for Italy_CA, Sardinia_Chalcolithic, Sardinia_EBA and Sardinia_Nuragic_BA. P-values for Sicily_EBA remained below 0.05 when either Iran_N (p-value=0.002) or Russia_Yamnaya_Samara (p-value=0.004) were added. Simultaneous modelling of Sicily_EBA with Iran_N and Russia_Yamnaya_Samara did also not improve the model fit (p-value=0.006) (**table S2.5**). We noticed that Sicily_EBA finds support in a three-source model (Anatolia_N, WHG and Yamnaya_Samara) when AHG is removed from the outgroups, or as four-source model (Anatolia_N, WHG, Yamnay_Samara, and Iran_N) when Morocco_Iberomaurusian is removed. Both outgroups share Levantine-like ancestry that is important in modelling Sicily_EBA (**table S2.5**).

To show that the third ancestry component that is required for Sardinian groups was related to Iran_N and not to steppe-related ancestry represented by Yamnaya_Samara, we rotated Iran_N to the outgroups and added Yamnaya_Samara as a third source. By doing so, the p-values for models of the central Mediterranean groups fell below 0.05. In turn, by adding Yamnaya_Samara to the outgroups and using Iran_N as additional source, the p-values remained high, indicative of a good model fit (≥0.05). We found consistent results between a competing three-way model and a rotating strategy and therefore conclude that there was an increase of Iran_N-like ancestry in Sardinia over time which became maximized in Sardinia_BA_Nuragic, and suggests a hidden Mediterranean gene flow rather than population continuity as has been suggested (*52*). Based on the currently available data, a genetic contribution from Italy is possible, where Iran_N-like ancestry has been shown to be present since the Neolithic (*50*). (**table S2.5)**.

7.1.3 Model 1c: Exploring genetic structure of SE_Iberia_CA

Target: Iberian MLN and CA groups
Sources: Anatolia_Neolithic, WHG, GoyetQ2 and either Iran_N, Russia_Yamnaya_Samara or Jordan_PPNB.
Outgroups: Mbuti.DG, Ethiopia_4500BP.SG, Ust_Ishim.DG, Russia_MA1_HG.SG, Italy_Villabruna, Belgium_GoyetQ116_1_published, Han.DG, Onge.DG, Papuan.DG, AHG, CHG, Morocco_Iberomaurussian.

In "Model 1a**"**, only SE_Iberia_CA groups did not find model support. Here, in model 1c we assume that the absence of subtle proportions of Yamnaya_Samara like ancestry in Iberia CA were the reason for the model failure. By adding Iran_N as an additional source we observed that the model fit improved (from p-value 0.009 to 0.014), whereas adding Yamnaya_Samara did not (p-value 0.005). However, we also detect a further improvement of the model fit when Jordan_PPNB is added as a fourth source (p-value=0.027) (**table S2.4**).

We then explored whether some of the *outgroups* are "breaking the model" for SE_Iberia_CA due to their importance as sources. We excluded Morocco_Iberomaurusian from the outgroups and tried to model SE_Iberia_CA with three (Anatolia, WHG and GoyetQ2) or four sources (Anatolia, WHG, GoyetQ2 and Morocco_Iberomaurusian), but this did not result in an improvement of the p-values (≥0.05). We proceeded in the same way with CHG and AHG. Intriguingly, we found that removing AHG from the outgroups increased the model fit when SE_Iberia_CA is modelled as three sources (Anatolia_Neolithic, WHG and GoyetQ2_review2, p-value= 0.045). Removing AHG from the set of outgroups also improves the fit in Sicily_EBA (Anatolia_Neolithic, WHG and Russia_Yamnaya_Samara, p-value = 0.115), whereas removing Morocco_Iberomaurusian and CHG does not change the p-values. It is therefore possible that the reasons for the unsuccessful attempts to model SE_Iberia_CA and Sicily_EBA, are different sources of early Neolithic ancestry but nonetheless are forming part of the same Mediterranean metapopulation. This further suggests that the position of SE_Iberia_CA in PC space is not only different from other northern CA groups because of remnant Magdalenian-like ancestry, but also due to an additional Mediterranean contribution, that differs from the baseline Anatolia_N ancestry in that it is more enriched for Iran_N-like ancestry. Indeed, a slightly different source of early farmer ancestry has been suggested as subtle but characteristic for the Mediterranean expansion of the Early Neolithic (*50*, *59*). (**fig. S3**). We also observed an excess of Iran_N-like

ancestry in Sardinia, but the results suggest that other different farming sources could spread along the Mediterranean at the same time. Geographically, it is plausible to assume a higher number of Neolithic ancestry sources during the Neolithic expansion in the Mediterranean when compared to central Europe, due to a direct contact to the Mediterranean Sea enabling higher mobility of early Neolithic groups.

8. Modelling ancestry in Bronze Age individuals

8.1 The arrival of the steppe-related ancestry in southern Iberia and its geographical gradient

We clearly detect the presence of steppe-related ancestry in all newly reported BA individuals (99 in total) and an almost complete turnover of Y-chromosome lineages in male individuals (**fig. 3B, table S2.6**). The result was further confirmed by using ADMIXTURE model-based clustering (*60*), where at k=8 we observed an additional ancestry component in all Iberian BA groups that is absent in all preceding Iberian CA groups. The new genetic component (visualized in green) is maximized in CHG and Iran_N individuals and also formed part of the Yamnaya_Samara group as distal source which stands for steppe ancestry, as well as all derived Late Neolithic and/or BA groups that carry steppe-related ancestry in admixed form (**fig. S4**). However, we also observed from PCA (**fig. 3A)** that the two well-represented Argaric sites (BAS with 8 individuals and ALM with 60, after excluding 1st degree relatives) appear to carry less steppe-related ancestry than other Iberian BA groups. We used *f4*-statistics of the form *f4*(N_Iberia_BA, test; Yamnaya_Samara, Mbuti) to show that the amount of steppe-related ancestry in Almoloya and Bastida was indeed significantly lower (**fig. S5A**, **table S2.7**). With the inclusion of the published northern and central Iberian CA individuals who show a higher amount of steppe-related ancestry, we confirmed that the amount of steppe-related ancestry followed a chronological and geographical gradient from North to South, with N_Iberia_BA and NE_Iberia_BA being the BA groups with the highest steppe-related ancestry component during BA (**fig. S5B, table S2.8**). In addition, the amount of steppe-related ancestry in the Balearic archipelago was higher than in the inland Iberian groups during LCA and BA (**fig. S5A** and **fig. S5B)**.

We used the method DATES (https://github.com/priyamoorjani/DATES) to estimate the admixture date between the Iberian local source (SE_Iberian_CA) and a Steppe-like related source (Yamnaya_Samara) in our BA groups from southeastern Iberia (**table S2.9**). DATES measures the ancestry covariance coefficient between pairs of SNPs along the chromosomes which shows a decay rate that is depending on the time of admixture. This method can be applied at individual level and assumes a single admixture event. The model used here shows that the admixture between local CA and Steppe-like related sources happened around 3.3 to 35 generations before, which equates to a range of calendar years from ~2550 BCE ± 189 years to ~1642 BCE ± 133 years (**table S2.9**) cal BCE, applying a generation time of 28 years (*93*).

By integrating the archaeological context of the first individuals with steppe-related ancestry in North and central Iberia, we can show that individuals with attested steppe-related ancestry (*7*) at sites such as El Hundido and Arroyal, are clearly intrusive in the collective burial monuments of the preceding phase. The detailed chronology of these cases of intrusive burials also suggests an

earlier arrival of steppe-related ancestry in northern Iberia (c. 2400 cal BCE) from where it had spread subsequently south by 2200 cal BCE.

8.2 Exploring Iran_N-like ancestry in Iberian BA individuals

The presence of steppe-related ancestry in Europe has been inferred by a displacement towards the PC2 (*4*), which broadly connects the European Neolithic populations (on the bottom) with populations from the Eurasian steppe such as Yamnaya_Samara (on the top). The shift from one to the other has been modeled and correlates well with the increasing amount of steppe-related ancestry. Thus, many studies have modelled LNBA populations using three distal sources (Anatolia_Neolithic, WHG and Yamnaya_Samara) (e.g. (*4*, *6*, *77*, *115*).

8.2.1 Models

8.2.1.1 Model 2 (**table S2.10**)

Target: Iberian_CA_Stp and Iberian BA groups
Sources: Anatolia_N, WHG, GoyetQ2, Iran_Ganj_Dareh_Neolithic or Yamnaya_Samara
3-way model: iterating Yamnaya Samara or Iran_Ganj_Dareh_Neolithic
4-way model: combining Anatolia_N, WHG, Yamnaya_Samara and Iran_Ganj_Dareh_Neolithic.
Outgroups: Mbuti.DG, Ethiopia_4500BP.SG, Ust_Ishim.DG, Russia_MA1_HG.SG, Italy_Villabruna, Belgium_GoyetQ116_1_published, Han.DG, Onge.DG, Papuan.DG, AHG, CHG, Morocco_Iberomaurusian

Please see **table S2.10** for detailed *qpWave* and *qpAdm* results.

We started estimating the amount of steppe-related ancestry using a distal model. This model was only applied to Iberian CA_Stp and BA groups with the aim to test whether the Magdalenian-associated component represented by GoyetQ2 was still detectable in the newly reported southern BA individuals. As in "Model 1" above, WHG included KO1 and Loschbour, to the exclusion of La Brana1.

Applying this model, we found that the regional substructure related to HG ancestry seen in CA groups was no longer detectable in Iberian BA groups ("Model 2", **table S2.10**). In turn, we excluded GoyetQ2 as a potential source and exchanged it by Iran_Ganj_Dareh_Neolithic to have a 4-way model combining Anatolia_N, WHG, Yamnaya_Samara and Iran_Ganj_Dareh_Neolithic. For most of the Iberian groups, we find model support using with Yamnaya_Samara as third source, while some Iberian groups can be modelled successfully using either Iran_N or Yamnaya_Samara as sources (e.g MolinosPapel_Early_Argar, SW_Iberia_BA and C_Iberia_BA_CogI). Interestingly, the three-source model does not work in some of the BA groups from SE Iberia such as Bastida_Argar, Almoloya Argar Early, Almoloya Argar Late, and SE_CabezoRedondo BA. Here, we needed to combine Yamnaya_Samara with Iran_N to improve the model fit in three of them (**fig. S6, table S2.10**). The observation that the model failed for only some of the SE Iberia BA groups suggests a degree of continuity of the SE Iberian CA component, irrespective of the arrival of the steppe-related ancestry.

We can explain this observation either by a potential additional source of Iran_N-like ancestry in Mediterranean groups that could have reached SE Iberia during the BA, or alternatively, by a distinguishable genetic substructure in CA groups that is still present in the BA period, and was only partially affected by the arrival of steppe-related ancestry. To further explore which Iberian BA groups had received excess central Mediterranean/Iran_N-rich ancestry in addition to a central European-derived source of steppe-related ancestry, we applied a more proximal model as follows.

8.2.1.2 Model 3 (**table S2.11**)

Target: Iberian_CA_Stp and Iberian BA groups
Sources: C_Iberia_CA/SE_Iberia_CA, Germany_Bell_Beaker and a list of 8 ancient Mediterranean/Iran_N-rich sources
Outgroups: Mbuti.DG, Ethiopia_4500BP.SG, Ust_Ishim.DG, Russia_MA1_HG.SG, Italy_Villabruna, Belgium_GoyetQ116_1_published, Han.DG, Onge.DG, Papuan.DG, AHG, CHG, Morocco_Iberomaurusian.

Please see **table S2.11** for detailed *qpWave* and *qpAdm* results.

This model was applied specifically to Iberian Bell Beakers with steppe-related ancestry and BA groups to explore potential Mediterranean/Iran_N-rich ancestry, which provide chronologically plausible scenarios to have contributed genetically to Iberian populations. Here, we fixed the central European steppe-like ancestry source represented by Germany Bell Beaker and tested a list of 10 ancient Mediterranean sources with Iran_N-like ancestry. The local source was represented by different geographical Iberian CA groups. However, in **fig. 4A** we chose to plot only SE_Iberia_CA as a local CA group for our study area, and C_Iberia_CA as the geographic region where the arrival of Steppe ancestry is first well-documented in Late CA. Additionally, these groups are the best represented ones in terms of number of individuals (SE_Iberia_CA=34 individuals; C_Iberia_CA=33 individuals), which allowed us a higher resolution analysis.

By iterating the local source, we observed that SE_Iberia_CA and N_Iberia_CA were not a well-fitting local proxy for all Iberian BA groups, probably due to an excess of Mediterranean/Iran_N-like ancestry already present in SE_Iberia_CA and a higher hunter-gatherer ancestry component in N_Iberia_CA (**table S2.11**). Instead, we found that C_Iberia_CA provides a better fit for most Iberian BA groups, and therefore used these individuals as a local reference, but still retain and show all possible combinations in **table S2.11** and **fig. 4A**. Of note, when we used NE_Iberia_CA as a local source all Iberian populations were supported, which shows that the power of resolution using this group is not sufficient to explore signals of substructure in CA groups. The number of individuals included in this geographical group is the smallest of the five geographical groups tested (n=12). C_Iberia_CA and Germany_Bell_Beaker were not sufficient to model all Iberian BA groups successfully, especially those from southeastern parts of Iberia, including all newly reported El Argar individuals from Almoloya (Early and Late) and Cabezo Redondo. Leveraging insights gained from the previous models, we performed competitive *qpAdm* modelling to explore the best candidates from a list of largely contemporaneous Mediterranean sources with elevated levels of Iran_N-related ancestry (**table S2.11**). While we were not able to single out a specific Mediterranean population, a contribution is nonetheless evident, as adding Iran_Seh_Gabi_Chalcolithic as a third source yields results in

support for all models that were previously rejected. The rest of the Mediterranean sources improve the model fit, however, not all of them reach a value of >0.05 in all Iberian BA groups (**table S2.11**)

Based on our previous findings, which suggest the presence of Mediterranean/Iran_N-like ancestry already in SE_Iberia_CA, we used the same model but iterated through different Iberian CA groups as a local baseline. By exchanging C_Iberia_CA with SE_Iberia_CA, we found two-way model support for Cabezo Redondo, suggesting that no Mediterranean source is needed, whereas models for Almoloya (Early and Late) can be rejected (**fig. 4, table S2.11**).

8.2.1.3 Model 4a **(table S2.12)**
Semi-distal model: local CA plus Yamnaya_Samara
Target: Iberian_CA_Stp and Iberian BA groups
Sources: N_Iberia_CA/C_Iberia_CA/SE_Iberia_CA, Yamnaya_Samara, and Iran_N/Jordan_PPNB
Outgroups: Mbuti.DG, Ethiopia_4500BP.SG, Ust_Ishim.DG, Russia_MA1_HG.SG, Italy_Villabruna, Belgium_GoyetQ116_1_published, Han.DG, Onge.DG, Papuan.DG, AHG,CHG, and Morocco_Iberomaurusian

Please see **table S2.12,** for detailed *qpWave* and *qpAdm* results.

In this model we fixed the source of 'steppe' ancestry with a distal proxy to explore the best local CA Iberian sources in modelling the geographically distinct Iberian BA groups. We used Yamnaya Samara as a distal proxy as have shown that CA_Stp and BA groups can be modelled successfully (Model 2), with the exception of Bastida_Argar, Almoloya_Argar_Early, Almoloya_Argar_Late, and SE_Cabezo_Redondo_BA. Maintaining the same set of outgrous as in Model 2 and 3, we explore the subtleties of the Neolithic ancestry in both models (AnatoliaN + WHG in model 2; or Iberia_CA in model 3) rather than the steppe-related ancestry, represented by Yamnaya_Samara, as we expect the latter contributing to all Iberian groups similarly.

By using C_Iberia_CA and Yamnaya_Samara as proxies, we could successfully model all Iberian BA groups with the exception of Almoloya_Argar_Early, Almoloya_Argar_Late and SE_CabezoRedondo_BA (same groups with the exception of Bastida that failed for the distal model 2 and 3). However, models for these three groups returned p-values ≥0.05 when Iran_N was added as a third source (**fig. S7**). Importantly, when we exchanged C_Iberia_CA by SE_Iberian_CA, most of the models failed, highlighting the genetic substructure among Iberian CA groups in line with **Supplementary Materials 7**. When Iran_N was added as a third source in combination of Yamnaya_Samara and SE_Iberia_CA, we always obtained a negative value for the Iran_N component, and these were considered "infeasible" models (**fig. S7**). However, the observation of systematically negative values suggests a shared ghost ancestry component in both Iran_N and in SE_Iberia_CA, which would be higher in SE_Iberia_CA. If the true admixture component is bigger in the source SE_Iberia_CA than in the target (each BA group), the model will show a poor fit in a two-way model. However, if the ghost admixture is bigger in our fixed source SE_Iberia_CA, the third source Iran_N results in a negative value in a three-way model. Our results are in line with this scenario.

Of note, SE_Iberia_CA as a source only works for SE Iberian BA groups, suggesting that first individuals with steppe-related ancestry are the result of local admixture with the different CA groups.

8.2.1.4 Model 4b (table S2.13)

Semi-proximal
Target: Iberian BA groups
Sources: C_Iberia_CA_Stp, C_Iberia_CA/SE_Iberia_CA and Iran_N (with one, two or three sources)
Outgroups: Mbuti.DG, Ethiopia_4500BP.SG, Ust_Ishim.DG, Russia_MA1_HG.SG, Italy_Villabruna, Belgium_GoyetQ116_1_published, Han.DG, Onge.DG, Papuan.DG, AHG, CHG and Morocco_Iberomaurusian

Please see **tables S2.13,** for detailed *qpWave* and *qpAdm* results.

The aim of this model is to explore temporally and geographically proximal sources to determine whether the Iran_N-rich/Mediterranean source missing in some BA groups is a true signal or, in turn, whether the use of proximal source results in sufficient model fit for SE Iberia BA groups. Using proximal CA sources as well as local steppe-related ancestry carrying individuals resulted in the same pattern as observed in Model 4a. The combination of C_Iberia_CA plus C_Iberia_CA_Stp required a third source in Almoloya_Argar_Early, Almoloya_Argar_Late, Bastida_Argar, SE_CabezoRedondo_BA and Aritges_LBA, that is best represented by distal Iran_N-like ancestry. However, this third source is not required when using SE_Iberia_CA, although we still do not get a fitting model for Almoloya_Argar_Early (p-value= 0.020) and Almoloya_Argar_Late (p-value=2.4E-04). This either shows the distinctive ancestry of La Almoloya individuals or the ability to detect such subtle signals only in well-covered groups consisting of a larger number of individuals as is the case for Almoloya_Argar_Early (n= 36) and Almoloya_Argar_Late (n=22). The improvement of the p-values in the two-source model when using SE_Iberia_CA instead of C_Iberia_CA is pointing again to a direct contribution of local CA groups to SE Iberian BA, which cannot be rejected in the case of Bastida. This could mean that Iran_N/Mediterranean-like ancestry was already present in SE_Iberia_CA groups (as is suggested in **Supplementary Materials 7**). In either case, we clearly observe that using the most proximal sources for the Iberian Peninsula is not enough to model Almoloya_Argar_Early and Almoloya_Argar_Late with satisfying statistical support as two-way models, which could either mean that the contribution of Iran_N/Mediterranean-like ancestry was sustained in time and persisted during BA, or that SE_Iberia_CA group does not represent well the ancestral population that inhabited SE Iberia during the CA.

8.2.1.5 Model 4c (tables S2.14)

Proximal
Target: SE Iberian BA groups
Sources: C_Iberia_CA_Stp, C_Iberia_CA/SE_Iberia_CA and central/eastern Mediterranean groups (Sicily_EBA, Sardinia_Nuragic_BA, Alalakh_MLBA, Italy_CA, Sardinia_EBA, Iran_Seh_Gabi_Chalcolithic, Greece_Minoan, Greece_Mycenaean, Greece_EBA, Greece_MBA)

Outgroups: Mbuti.DG, Ethiopia_4500BP.SG, Ust_Ishim.DG, Russia_MA1_HG.SG, Italy_Villabruna, Belgium_GoyetQ116_1_published, Han.DG, Onge.DG, Papuan.DG, AHG, CHG and Morocco_Iberomaurusian, Iran_N

Please see **tables S2.14,** for detailed *qpWave* and *qpAdm* results.

This model was applied specifically to Almoloya_Argar_Early and Almoloya_Argar_Late groups. Here, we exchanged Iran_N by central and eastern Mediterranean groups that are potential candidates for Iran_N-enriched proximal sources, and thus moved Iran_N to the outgroups. However, this did also not result in a good model fit for Almoloya_Argar_Early and Almoloya_Argar_Late, we found that the qpWave value decreases in nine orders of magnitude when C_Iberia_CA_Stp, SE_Iberia_CA and Sicily_EBA are tested as sources (p-value =1.14038495e-17), compared to using C_Iberia_CA as local source in the same three-way model (p-value =4.66848228e-26). A similar decrease of qpWave values was observed when using other central Mediterranean groups such as Sardinia_EBA (**table S2.14**). Since the CA source is the unique variable changing in the qpWave model, we assume that SE_Iberia_CA is overall more similar to Sicily_EBA and other central Mediterranean groups than C_Iberia_CA. This result is also indicative of a marked CA substructure and higher Mediterranean influence in SE_Iberia_CA. Another indication for shared common ancestry between Sicily_EBA and SE_Iberia_CA is the observation of non-feasible 3-way models. When we modelled Amoloya_Argar_Early and Late as three sources with C_Iberia_CA_Stp, SE_Iberia_CA and Central/Easter Mediterranean population, we obtain negative results for Sicily_EBA, which indirectly highlights a shared common ancestry with SE_Iberia_CA.

8.2.1.6 Model 4d (table S2.15)

Rotating semi-proximal sources
Target: Iberian BA groups
Sources: C_Iberia_CA_Stp, C_Iberia_CA and Iran_N
Outgroups: Mbuti.DG, Ethiopia_4500BP.SG, Ust_Ishim.DG, Russia_MA1_HG.SG, Italy_Villabruna, Belgium_GoyetQ116_1_published, Han.DG, Onge.DG, Papuan.DG, AHG, CHG and Morocco_Iberomaurusian (plus Sicily_EBA, Sardinia_Nuragic_BA, Alalakh_MLBA, Italy_CA, Sardinia_EBA, Greece_Minoan, Greece_Mycenaean, Greece_EBA, Greece_MBA and Germany_Bell_Beaker rotated one by one)

Please see **table S2.15,** for detailed *qpWave* and *qpAdm* results.

In order to get a general idea about the missing source in south eastern Iberian BA groups, we took the three-way model which worked best for all Iberian groups (C_Iberia_CA_Stp, C_Iberia_CA and Iran_N) and rotated through a set of populations from central Europe (Germany_Bell_Beaker), the central Mediterranean (Sicily_EBA, Sardinia_Nuragic_BA, Italy_CA, Sardinia_EBA, Greece_Minoan, Greece_Mycenaean, Greece_EBA and Greece_MBA), and the eastern Mediterranean (Alalakh_MLBA) in the outgroups. The aim of this strategy was to evaluate which population "breaks" the model fit, which would imply that ancestry represented by tested population in the outgroup is more directly related to the target (south eastern Iberia BA groups) than to the sources (either C_Iberia_CA_Stp, C_Iberia_CA and Iran_N). By using this strategy we observed that Sicily_EBA is the only population in 1240k

capture data format (when used in the outgroups), which makes the model fail for Almoloya_Argar_Early (p-value=0.023) and decreases the p-value for Almoloya_Argar_Late (p-value=0.050), whereas without Sicily_EBA in the outgroups Almoloya_Argar_Early and Almoloya_Argar_Late can be successfully modeled with three sources (p-value=0.119 and 0.092, respectively). Of note, having Greece_EBA and Greece_MBA (SG data format) in the outgroup, also decreases the model fit for Almoloya_Argar_Early and Almoloya_Argar_Late. Using other groups as outgroups also improves the model fit, and increases the p-values for both El Argar groups above 0.10 in all combinations (**Table S2.15**).
Taken together, these modelling attempts point to two sources of newly emerging ancestry in BA Iberia: a group with central European-derived steppe-related ancestry, and in parallel a Mediterranean influence carrying excess Iran_N-like ancestry, which might have arrived already during the Copper Age in SE Iberia and which is likely independent of the spread of steppe-related ancestry. The detectable Iran_N-rich ancestry in early and late El Argar phases in SE Iberia is supported by both proximal and distal models and suggests either continuous contact with the Mediterranean world or a second pulse of influence during the El Argar Bronze Age. A denser regional sampling of Bell Beaker and BA individuals from regions in today's France and Italy as well as the eastern Mediterranean and North Africa will no doubt shed further light on how the Mediterranean was connected not only in trading but also genetically.

9. The outlier Zapatería individual (ZAP002)
The position of individual ZAP002 in the PCA plot identified him as a genetic outlier in comparison to other El Argar individuals. Applying different f4-statistics, we could formally test and confirm the presence of North African ancestry (**fig. 5A** and **fig. 5B**). As a consequence, we were aiming to quantify these ancestral sources with *qpAdm* modelling.

9.1 Modelling the ancestry of ZAP0002
To be able to compare results directly with the previous models applied to other El Argar individuals, we kept the same set of outgroups for the ancestry modelling of ZAP002.

9.1.1 Model 5a **(table S2.18)**
Target: ZAP002
Sources: C_Iberia_CA/SE_Iberia_CA/central Mediterranean groups and Germany_Bell_Beaker
Outgroups: Mbuti.DG, Ethiopia_4500BP.SG, Ust_Ishim.DG, Russia_MA1_HG.SG, Italy_Villabruna, Belgium_GoyetQ116_1_published, Han.DG, Onge.DG, Papuan.DG, AHG, CHG, Morocco_Iberomaurusian

Please see **table S2.18** for detailed *qpWave* and *qpAdm* results.

Applying **"**Model 5a**"** we did not find any model fit, which is due to having Morocco_Iberomaurusian in the outgroups in the starting model for reason of being fully comparable at the outset. Thus, the African ancestry in Morocco_Iberomaurusian is more likely needed as a source, as shown in f4-statistics (**fig. 5A** and **fig. 5B**).

9.1.2 Model 5b **(table S2.18)**
Target: ZAP002

Sources: SE_Iberia_CA/C_Iberia_CA/central Mediterranean groups, Germany_Bell_Beaker and Morocco Iberomaurusian.
Outgroups: Mbuti.DG, Ethiopia_4500BP.SG, Ust_Ishim.DG, Russia_MA1_HG.SG, Italy_Villabruna, Belgium_GoyetQ116_1_published, Han.DG, Onge.DG, Papuan.DG, AHG, CHG

Please see **table S2.18** for detailed *qpWave* and *qpAdm* results.

In order to investigate a potential non-local ancestry contribution in individual ZAP002, we applied the following competitive "Model 5b**"**.

We show that Morocco Iberomaurusian is needed as a third source to improve the model fit. Interestingly, we also found that the local Iberian ancestry, represented by C_Iberia_CA or SE_Iberia_CA, is not needed to obtain a p-value ≥0.05, whereas all models with central Mediterranean sources are supported, among which the one with Sicily_EBA yielded the highest p-value (**table S2.18**).

9.1.3 Model 5c **(table S2.18)**
Target: ZAP002
Sources: central Mediterranean groups, Germany_Bell_Beaker and Morocco_Iberomaurusian
Outgroups: Mbuti.DG, Ethiopia_4500BP.SG, Ust_Ishim.DG, Russia_MA1_HG.SG, Italy_Villabruna, Belgium_GoyetQ116_1_published, Han.DG, Onge.DG, Papuan.DG, AHG, CHG, C_Iberia_CA

In "Model 5c**"** we moved C_Iberia_CA to the outgroups to explore a rotating model. By doing so, all models including a central Mediterranean source retained p-values ≥0.05. On the basis of these results, we concluded that individual ZAP002 is highly likely a non-local individual, who carries steppe-related, central Mediterranean and North African ancestries.

10. Phenotypic and functional variants

We explored 41 SNPs related to physical appearance (skin, eye or hair color) and we used HIrisPlex-S to predict the probability among phenotypes (**fig. S8, table S2.19**). The model uses the variants to estimate the highest probability value for a predicted phenotype. Apart from our cutoff in 400,000 SNPs covered in the 1240k panel, the model only predicts phenotypes in individuals with input SNPs in genes HERC2 (rs12913832) to predict eye color, MC1R (11 SNPs located in the gene) to predict hair color, and HERC2-SLC45A2-IRF4 to predict both eye and hair color (https://hirisplex.erasmusmc.nl). Despite the differences in the numbers of analyzed individuals for the Copper Age and the Bronze Age, individuals with blue eyes were absent in the Bronze Age individuals set. The rest of variety in skin, hair and/or eye colour were present in both Copper and Bronze age individuals (**fig. S8, table S2.19**).
Apart from the SNPs involved in skin and hair pigmentation and eye color, we also explored 14 SNPs distributed along eight genes linked to the ability to digest lactose (snp_2_136608574, snp_2_136608642, rs41525747, rs4988236, rs4988235, rs41456145, rs41380347 and rs145946881 in *LCT*) and alcohol (rs1229984 in ADH1B), adaptation to metabolize fatty acids

(rs174546 in FADS1), predisposition to celiac disease (rs272872 in SLC22A4 and rs653178 in ATXN2/SH2B3) or resistance to infectious diseases (rs4833103 in the gene cluster TLR1-TLR6-TLR10 and rs2269424 in the Major Histocompatibility Complex (MHC)). For each locus, we report the frequencies of the derived alleles in total reads covered on this site, analyzing CA and BA individually in two separate groups. We found no significant differences in frequency of the derived alleles between the CA and BA groups (**fig. S9, table S2.20**).

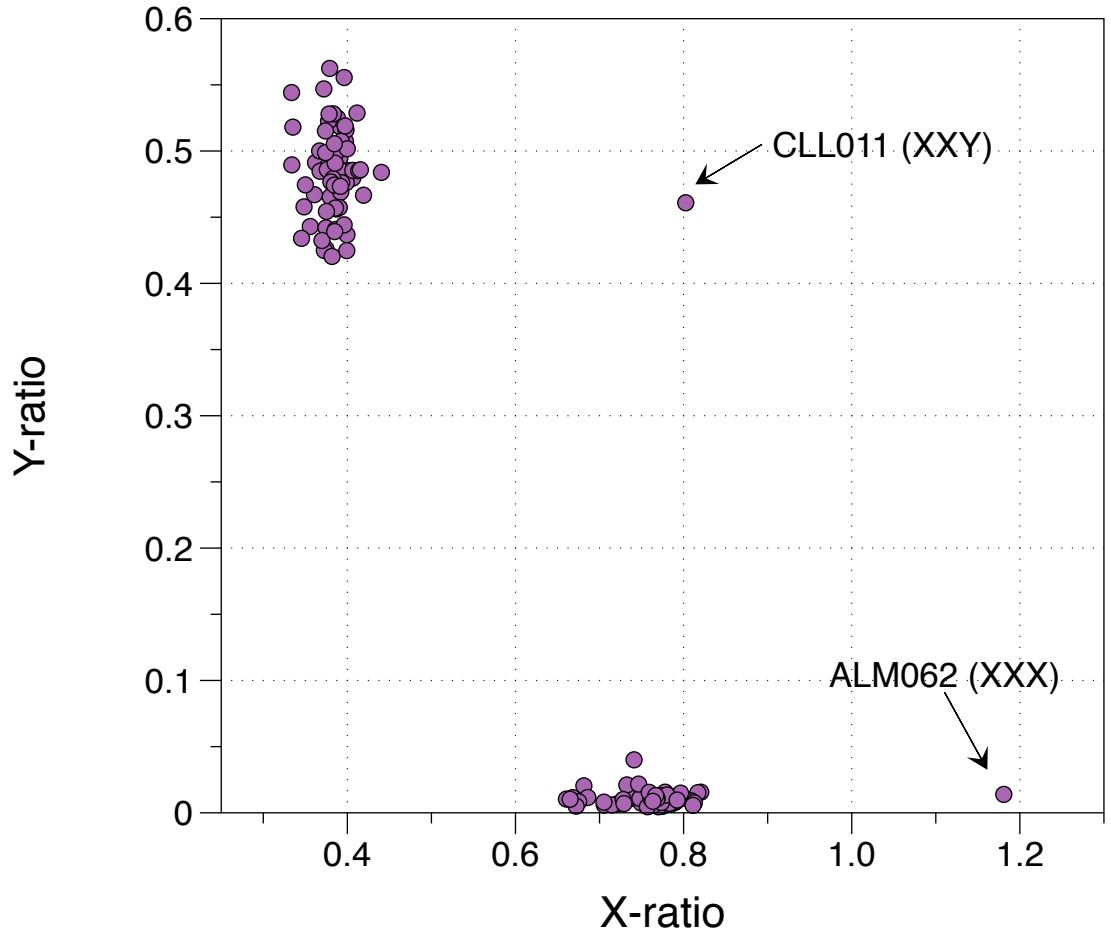

Fig. S1. Scatter plot for X and Y- ratio of the analyzed individuals, including CLL011 (XXY) who shows a X-ratio compatible with genetic females and Y-ratio compatible with genetic males and ALM062 (XXX) with a X-ratio compatible with 0.5 times higher than the female X-ratio.

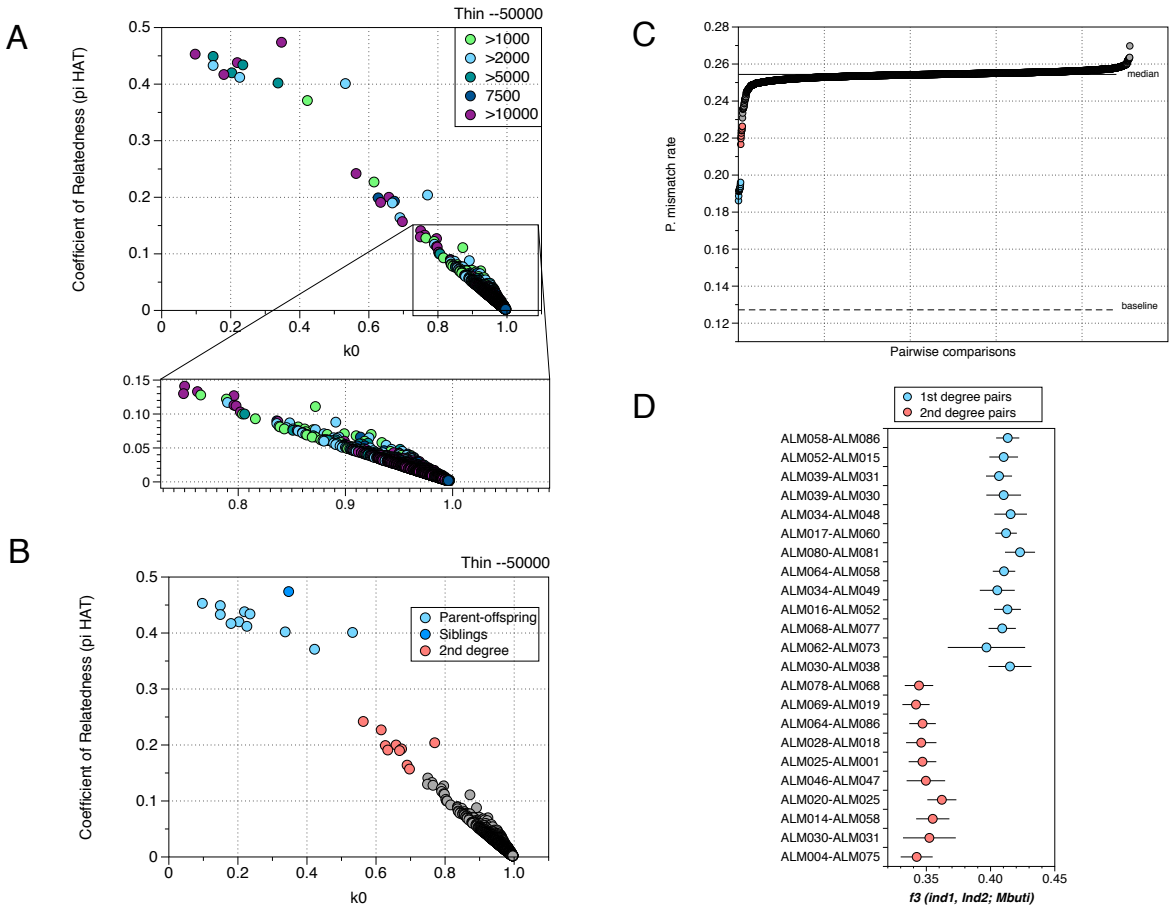

Fig. S2. Comparison of kinship methods to infer the degree of relatedness among individuals from the site La Almoloya. (**A**) Coefficient of Relatedness versus k0 for pairs of individuals with at least 1000 shared SNPs calculated with LcMLkin (colors indicate SNP coverage) (**table S1.7**); (**B**) Coefficient of Relatedness versus k0, highlighting 1st (blue) and 2nd(red) degree pairs of individuals with at least 1000 shared SNPs (**table S1.7**); (**C**) Pairwise mismatch rate (PWMR) for individuals with at least 1000 shared SNPs highlighting 1st (blue) and 2nd (red) degree pairs (**table S1.5**); (**D**) Significantly positive f3-outgroup statistics for all 1st and 2nd degree pairs confirming the separation of the two groups.

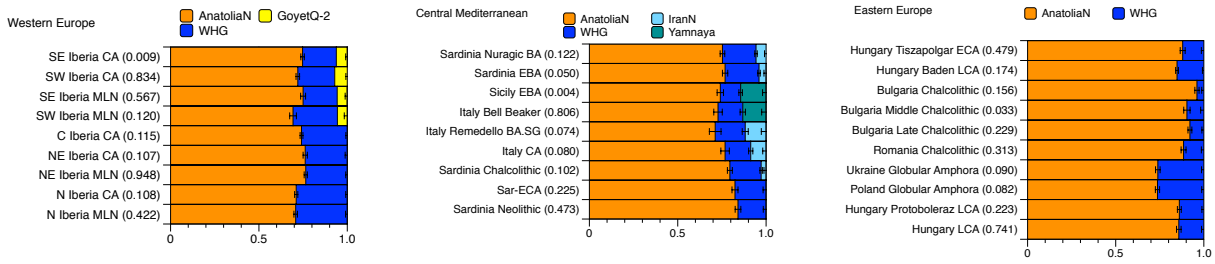

Fig. S3. qpAdm admixture models for western European, central Mediterranean and eastern European CA and EBA groups using distal sources Anatolia_N, WHG, GoyetQ2 and Iran_N (Supplementary Materials 7, table S2.4 and table S2.5).

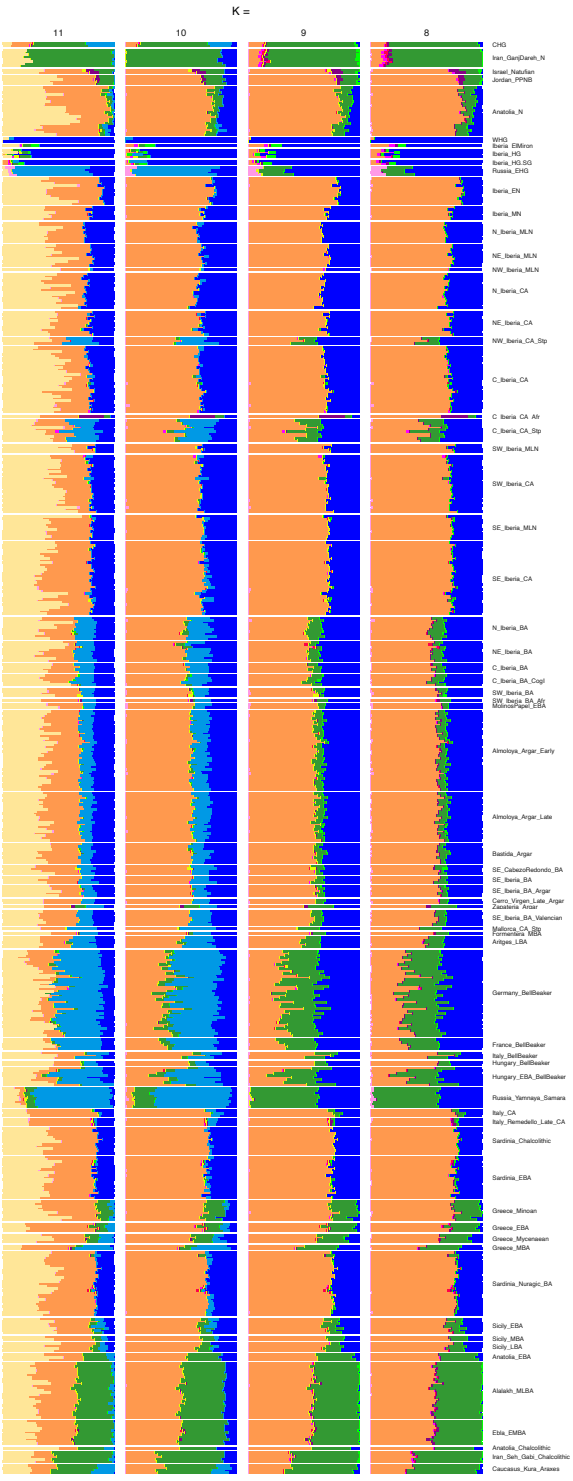

Fig. S4. Results of the ADMIXTURE cluster analysis. We show a subset of ancient individuals for k=8-11, which represents individuals and groups mentioned in the main text, which are used for quantitative modelling approaches and in which relevant ancestry components are maximized**.**

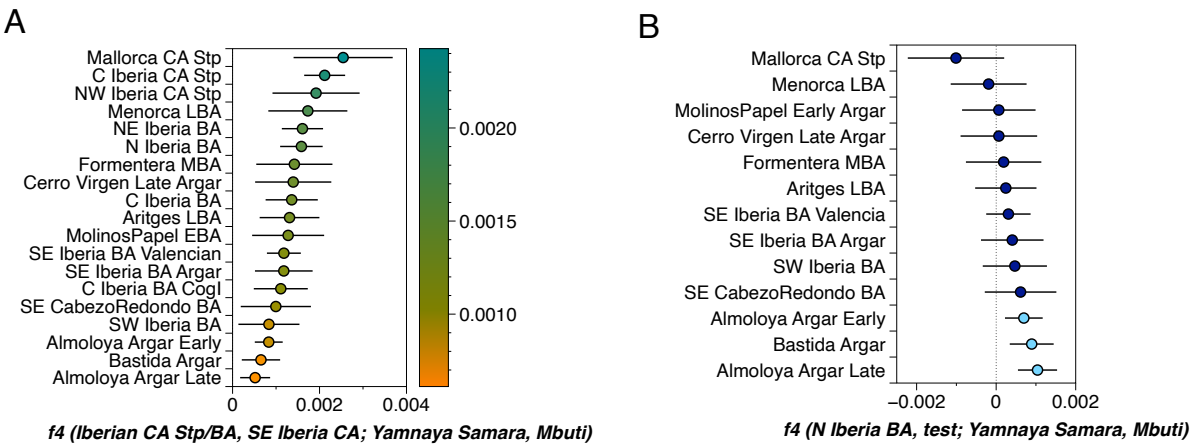

Fig. S5. Gradient of steppe-related ancestry in Iberian BA individuals. (A) f4-statistics showing the presence of steppe-related ancestry in all the newly reported BA groups, confirming a gradient from north (higher steppe-related ancestry) to south (lower steppe-related ancestry) (**table S2.7**). A temporal decrease of steppe-related ancestry on the Balearic Islands is seen between Mallorca_CA_Stp and Menorca_LBA, Formentera_MBA and Aritges LBA, in line with (*51*); **(B)** f4-statistics contrasting north Iberian BA group with newly reported southern groups, which shows the significantly smaller amount of steppe-related ancestry in individuals from Almoloya and Bastida. Light blue colors indicate a Z-score of > 3. **(table S2.8).**

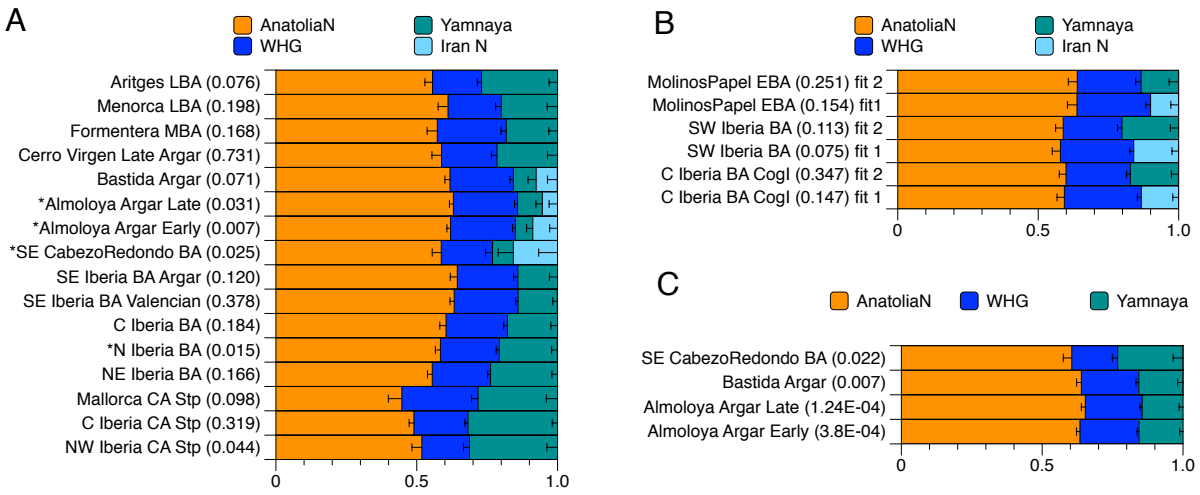

Fig. S6. qpAdm admixture modelling of Iberian BA groups using distal sources Anatolia_N, WHG, Yamnaya_Samara, and Iran_Ganj_Dareh_Neolithic. (A) Groups that can only be modelled with Yamnaya Samara, or with a combination of Yamnaya Samara and Iran N (nested models with higher p-values are plotted; asterisks indicate rejected models based on a p-value cut off of < 0.05) (**table S2.10, Supplementary Materials 8**), and **(B)** Groups that can be modelled either with Iran_N or Yamnaya_Samara as a third source (with Yamnaya_Samara usually showing the higher p-value). **(C)** qpAdm of the rejected 3-way model using Anatolia_N, WHG and Yamnaya_Samara as distal sources.

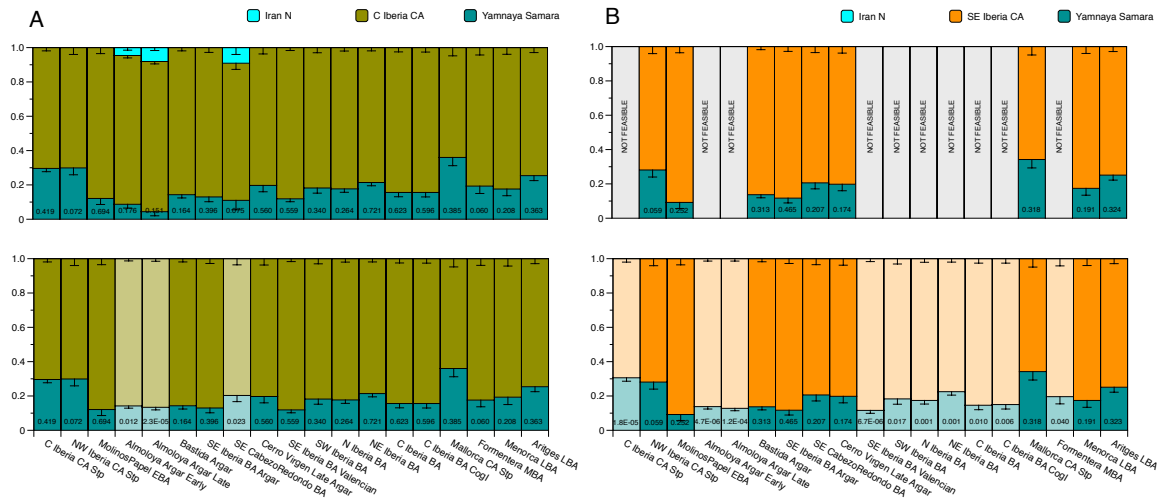

Fig. S7. Modelling Iberian BA and CA individuals with steppe-related ancestry as a two- and three-way qpAdm admixture. (A) qpAdm admixture model using proximal CA source C_Iberia_CA, Yamnaya_Samara and Iran_N; **(B)** qpAdm admixture model using proximal CA source SE_Iberia_CA, Yamnaya_Samara and Iran_N. Two-way models that find no support are faded out. Three-way infeasible models are shown as "Not feasible" (**table S2.12**).

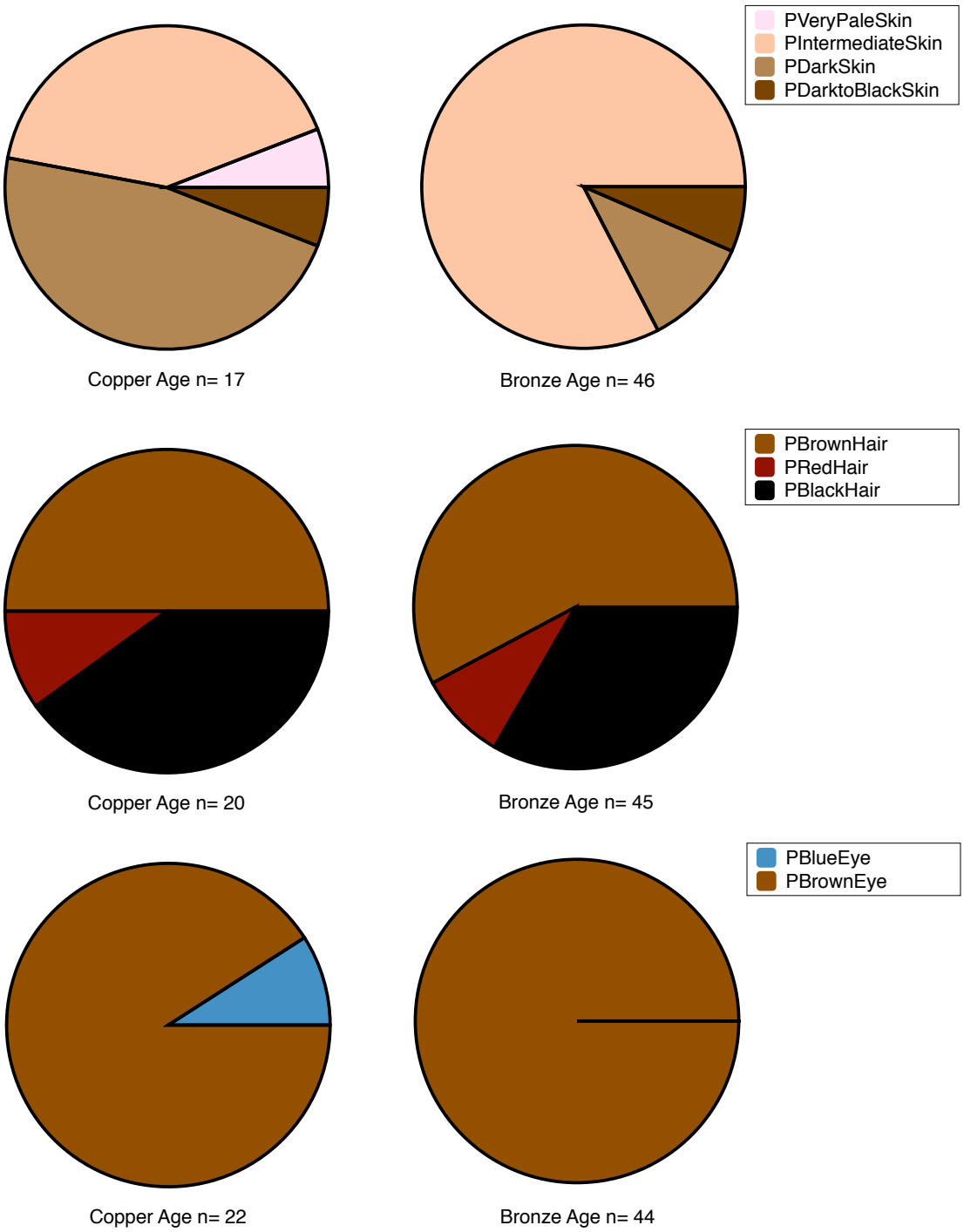

Fig. S8. Predicted phenotypes (skin color, hair color and eye color) using HIrisPlex-S (*89*, *116*, *117*) for Copper Age and Bronze Age individuals with more than 400,000 SNPs coverage in 1240k panels (table S2.19).

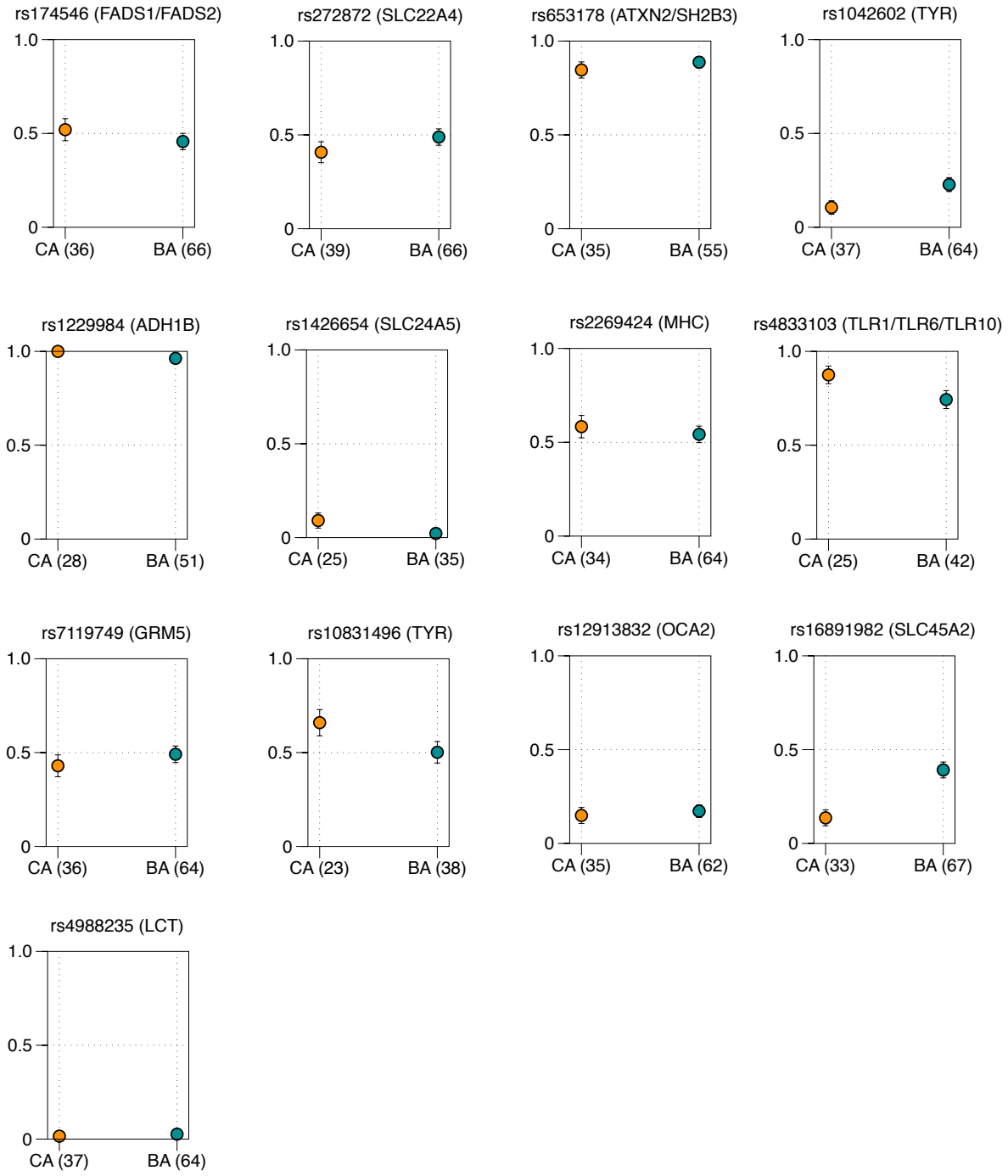

Fig. S9. Estimated allele frequency for 13 phenotypic SNPs. We show the maximum likelihood frequency estimates and 1SE for the derived allele frequency in CA (orange) and BA (dark green) groups, with the number of individuals in brackets (**table S2.20**).

Table S1. Descriptive summaries of genomic results:
S1.1. Archaeological context and main genomic data (fig. 1);
S1.2. 1240k EAGER data;
S1.3. Mitocapture EAGER data;
S1.4. Mitochondrial haplogroup assignment;
S1.5. Pairwise mismatch rate (PWMR) analysis (fig. S2C);
S1.6. READ analysis;
S1.7. lcMLkin analysis (fig. S2A, fig. S2B).

Table S2. Details of genomic data analyses:
S2.1. Group labels and comparative ancient dataset used in this study;
S2.2. f4-statistics showing significant differences in terms of WHG ancestry in northern and southern MLN and CA groups (fig. 2B);
S2.3. f4-statistics highlighting the higher affinity of Southern MLN and CA Iberian groups to Goyet Q-2 (fig. 2C);
S2.4. Modelling Iberian MLN and CA without Steppe ancestry (fig. 2D);
S2.5. Modelling Central Mediterranean and Eastern Europe CA and EBA (fig. S1);
S2.6. f4-statistics testing for a geographic gradient of steppe ancestry in Iberia (fig. S3A);
S2.7. f4-statistics testing for significant differences in steppe ancestry among geographical groups in Iberia (fig. S3B);
S2.8. Individual f4-statistics showing the increased affinity to Yamanaya_Samara during the EBA, absent in CA individuals and Y-chromosome haplogroups (fig. 3B);
S2.9. Admixture dating of local and Steppe ancestries with DATES;
S2.10. Distal Model 2 for CA Iberian Stp and Iberia BA (fig. S4);
S2.11. Bell-beaker model (Model 3) for CA Iberian Stp and Iberia BA (fig. 4A);
S.2.12. Semi-distal admixture modelling of CA Iberian Stp and Iberia BA (Model 4a, fig. S5);
S2.13. Semi-proximal admixture modelling of CA Iberian Stp and Iberia BA (Model 4b, fig. 4B);
S2.14. Proximal admixture modelling of Iberia BA (Model 4c);
S2.15. Rotating strategy in semi-proximal admixture modelling of Iberia BA (Model 4d);
S2.16. f4-statistics testing for North African ancestry in ZAP002 outlier (fig. 5A);
S2.17. f4-statistics testing for North African or Basal Eurasian ancestry in ZAP002 outlier (fig. 5B);
S2.18. ZAP002 outlier admixture modelling (Model 5a and Model 5b) (fig. 5C);
S2.19. Physical appearance with HirisPlex (fig. S7);
S2.20. Estimated allele frequency for phenotypic SNPs (fig. S8);
S2.21. Runs of homozygosity using HapROH (fig. 6A);
S2.22. Sex bias (fig. 6B);
S2.23. Testing for skewness in f3-outgroup male-male, female-female and female-male (fig.6C);
S2.24. Testing for patrilocality via mean pairwise mismatch rate (fig. 6D).

REFERENCES AND NOTES

1. H. Weiss, M.-A. Courty, W. Wetterstrom, F. Guichard, L. Senior, R. Meadow, A. Curnow, The genesis and collapse of third millennium north Mesopotamian civilization. *Science* **261**, 995–1004 (1993).

2. C. Kuzucuoğlu, C. Marro, *Sociétés Humaines Et Changement Climatique À la Fin Du Troisième Millénaire: Une Crise A-t-elle Eu Lieu en Haute Mésopotamie?: Actes Du Colloque de Lyon, 5–8 Décembre 2005* (Institut français d'études anatolienne Georges-Dumézil, 2007).

3. H. Meller, H. W. Arz, R. Jung, R. Risch, *2200 BC—A Climatic Breakdown as a Cause for the Collapse of the Old World?* (Tagungen des Landesmuseums für Vorgeschichte Halle, 12. Landesamt für Denkmalpflege und Archäologie Sachsen-Anhalt, Landesmuseum für Vorgeschichte, 2015).

4. W. Haak, I. Lazaridis, N. Patterson, N. Rohland, S. Mallick, B. Llamas, G. Brandt, S. Nordenfelt, E. Harney, K. Stewardson, Q. Fu, A. Mittnik, E. Bánffy, C. Economou, M. Francken, S. Friederich, R. G. Pena, F. Hallgren, V. Khartanovich, A. Khokhlov, M. Kunst, P. Kuznetsov, H. Meller, O. Mochalov, V. Moiseyev, N. Nicklisch, S. L. Pichler, R. Risch, M. A. Rojo Guerra, C. Roth, A. Szécsényi-Nagy, J. Wahl, M. Meyer, J. Krause, D. Brown, D. Anthony, A. Cooper, K. W. Alt, D. Reich, Massive migration from the steppe was a source for Indo-European languages in Europe. *Nature* **522**, 207–211 (2015).

5. M. E. Allentoft, M. Sikora, K.-G. Sjögren, S. Rasmussen, M. Rasmussen, J. Stenderup, P. B. Damgaard, H. Schroeder, T. Ahlström, L. Vinner, A.-S. Malaspinas, A. Margaryan, T. Higham, D. Chivall, N. Lynnerup, L. Harvig, J. Baron, P. D. Casa, P. Dąbrowski, P. R. Duffy, A. V. Ebel, A. Epimakhov, K. Frei, M. Furmanek, T. Gralak, A. Gromov, S. Gronkiewicz, G. Grupe, T. Hajdu, R. Jarysz, V. Khartanovich, A. Khokhlov, V. Kiss, J. Kolář, A. Kriiska, I. Lasak, C. Longhi, G. McGlynn, A. Merkevicius, I. Merkyte, M. Metspalu, R. Mkrtchyan, V. Moiseyev, L. Paja, G. Pálfi, D. Pokutta, Ł. Pospieszny, T. D. Price, L. Saag, M. Sablin, N. Shishlina, V. Smrčka, V. I. Soenov, V. Szeverényi, G. Tóth, S. V. Trifanova, L. Varul, M. Vicze, L. Yepiskoposyan, V. Zhitenev, L. Orlando, T. Sicheritz-Pontén, S. Brunak, R. Nielsen, K. Kristiansen, E. Willerslev, Population genomics of Bronze Age Eurasia. *Nature* **522**, 167–172 (2015).

6. I. Olalde, S. Brace, M. E. Allentoft, I. Armit, K. Kristiansen, T. Booth, N. Rohland, S. Mallick, A. Szécsényi-Nagy, A. Mittnik, E. Altena, M. Lipson, I. Lazaridis, T. K. Harper, N. Patterson, N. Broomandkhoshbacht, Y. Diekmann, Z. Faltyskova, D. Fernandes, M. Ferry, E. Harney, P. de Knijff, M. Michel, J. Oppenheimer, K. Stewardson, A. Barclay, K. W. Alt, C. Liesau, P. Ríos, C. Blasco, J. V. Miguel, R. M. García, A. A. Fernández, E. Bánffy, M. Bernabò-Brea, D. Billoin, C. Bonsall, L. Bonsall, T. Allen, L. Büster, S. Carver, L. C. Navarro, O. E. Craig, G. T. Cook, B. Cunliffe, A. Denaire, K. E. Dinwiddy, N. Dodwell, M. Ernée, C. Evans, M. Kuchařík, J. F. Farré, C. Fowler, M. Gazenbeek, R. G. Pena, M. Haber-Uriarte, E. Haduch, G. Hey, N. Jowett, T. Knowles, K. Massy, S. Pfrengle, P. Lefranc, O. Lemercier, A. Lefebvre, C. H. Martínez, V. G. Olmo, A. B. Ramírez, J. L. Maurandi, T. Majó, J. I. McKinley, K. McSweeney, B. G. Mende, A. Modi, G. Kulcsár, V. Kiss, A. Czene, R. Patay, A. Endrődi, K. Köhler, T. Hajdu, T. Szeniczey, J. Dani, Z. Bernert, M. Hoole, O. Cheronet, D. Keating, P. Velemínský, M. Dobeš, F. Candilio, F.

Brown, R. F. Fernández, A.-M. Herrero-Corral, S. Tusa, E. Carnieri, L. Lentini, A. Valenti, A. Zanini, C. Waddington, G. Delibes, E. Guerra-Doce, B. Neil, M. Brittain, M. Luke, R. Mortimer, J. Desideri, M. Besse, G. Brücken, M. Furmanek, A. Hałuszko, M. Mackiewicz, A. Rapiński, S. Leach, I. Soriano, K. T. Lillios, J. L. Cardoso, M. P. Pearson, P. Włodarczak, T. D. Price, P. Prieto, P.-J. Rey, R. Risch, M. A. Rojo Guerra, A. Schmitt, J. Serralongue, A. M. Silva, V. Smrčka, L. Vergnaud, J. Zilhão, D. Caramelli, T. Higham, M. G. Thomas, D. J. Kennett, H. Fokkens, V. Heyd, A. Sheridan, K.-G. Sjögren, P. W. Stockhammer, J. Krause, R. Pinhasi, W. Haak, I. Barnes, C. Lalueza-Fox, D. Reich, The Beaker phenomenon and the genomic transformation of northwest Europe. *Nature* **555**, 190–196 (2018).

7. I. Olalde, S. Mallick, N. Patterson, N. Rohland, V. Villalba-Mouco, M. Silva, K. Dulias, C. J. Edwards, F. Gandini, M. Pala, P. Soares, M. Ferrando-Bernal, N. Adamski, N. Broomandkhoshbacht, O. Cheronet, B. J. Culleton, D. Fernandes, A. M. Lawson, M. Mah, J. Oppenheimer, K. Stewardson, Z. Zhang, J. M. Jiménez Arenas, I. J. Toro Moyano, D. C. Salazar-García, P. Castanyer, M. Santos, J. Tremoleda, M. Lozano, P. García Borja, J. Fernández-Eraso, J. A. Mujika-Alustiza, C. Barroso, F. J. Bermúdez, E. Viguera Mínguez, J. Burch, N. Coromina, D. Vivó, A. Cebrià, J. M. Fullola, O. García-Puchol, J. I. Morales, F. X. Oms, T. Majó, J. M. Vergès, A. Díaz-Carvajal, I. Ollich-Castanyer, F. J. López-Cachero, A. M. Silva, C. Alonso-Fernández, G. Delibes de Castro, J. Jiménez Echevarría, A. Moreno-Márquez, G. Pascual Berlanga, P. Ramos-García, J. Ramos-Muñoz, E. Vijande Vila, G. Aguilella Arzo, Á. Esparza Arroyo, K. T. Lillios, J. Mack, J. Velasco-Vázquez, A. Waterman, L. Benítez de Lugo Enrich, M. Benito Sánchez, B. Agustí, F. Codina, G. de Prado, A. Estalrrich, Á. Fernández Flores, C. Finlayson, G. Finlayson, S. Finlayson, F. Giles-Guzmán, A. Rosas, V. Barciela González, G. García Atiénzar, M. S. Hernández Pérez, A. Llanos, Y. Carrión Marco, I. Collado Beneyto, D. López-Serrano, M. Sanz Tormo, A. C. Valera, C. Blasco, C. Liesau, P. Ríos, J. Daura, M. J. de Pedro Michó, A. A. Diez-Castillo, R. Flores Fernández, J. Francès Farré, R. Garrido-Pena, V. S. Gonçalves, E. Guerra-Doce, A. M. Herrero-Corral, J. Juan-Cabanilles, D. López-Reyes, S. B. McClure, M. Merino Pérez, A. Oliver Foix, M. Sanz Borràs, A. C. Sousa, J. M. Vidal Encinas, D. J. Kennett, M. B. Richards, K. Werner Alt, W. Haak, R. Pinhasi, C. Lalueza-Fox, D. Reich, *Science* **363**, 1230–1234 (2019).

8. V. Lull, R. Micó, C. Rihuete Herrada, R. Risch, *Transition and Conflict at the End of the 3rd Millennium BC in South Iberia*, H. Meller, H. W. Arz, R. Jung, R. Risch, Eds. (Landesmuseum für Vorgeschichte, 2015).

9. R. Chapman, *Archaeologies of Complexity* (Routledge, 2003).

10. P. B. Ramírez, J. A. Soler Díaz, *Ídolos: Miradas Milenarias* (Museo Arqueológico de Alicante, 2020).

11. M. D.-Z. Bonilla, J. Beck, H. Bocherens, P. Díaz-del-Río, Isotopic evidence for mobility at large-scale human aggregations in Copper Age Iberia: The mega-site of Marroquíes. *Antiquity* **92**, 991–1007 (2018).

12. A. C. Valera, I. Žalaitė, A. F. Maurer, V. Grimes, A. M. Silva, S. Ribeiro, J. F. Santos, C. Barrocas Dias, Addressing human mobility in Iberian Neolithic and Chalcolithic ditched enclosures: The case of Perdigões (South Portugal). *J. Archaeol. Sci. Rep.* **30**, 102264 (2020).

13. A. Banerjee, J. A. López Padilla, T. X. Schumacher, Marfil y elefantes en la Península Ibérica y el Mediterráneo occidental, *Iberia Archaeologica 16.1.* (Zabern, 2012).

14. T. X. Schuhmacher, Frühbronzezeitliche Kontakte im westlichen und zentralen Mittelmeerraum und die Rolle der Iberischen Halbinsel. *Madrider Mitteilungen* **45**, 147–180 (2004).

15. T. X. Schuhmacher, Elfenbeinobjekte des Chalkolithikums und der Frühen Bronzezeit auf der Iberischen Halbinsel. *Studien zu Herkunft, Austausch, Verarbeitung und sozialer Bedeutung von Elfenbein. Iberia Archaeologica* **16**, 610 (2012).

16. M. Murillo-Barroso, M. Martinón-Torres, Amber sources and trade in the prehistory of the Iberian peninsula. *Eur. J. Archaeol*. **15**, 187–216 (2012).

17. R. J. Harrison, A. Gilman, Trade in the second and third millennia BC between the Maghreb and Iberia, in *Ancient Europe and the Mediterranean: studies in honour of Hugh Hencken*, V. Markotic, Ed. (Aris & Phillips, 1977), pp. 90–104.

18. V. Hurtado Pérez, L. García Sanjuán, Los inicios de la Jerarquización Social en el Suroeste de la Península Ibérica (c. 2500–1700 ane): Problemas conceptuales y empíricos (1997); http://roderic.uv.es/bitstream/handle/10550/29498/2134.pdf?sequence=1.

19. R. Chapman, Producing inequalities: Regional sequences in later prehistoric Southern Spain. *J. World Prehist.* **21**, 195–260 (2008).

20. P. Díaz del Río, Labor in the making of Iberian Copper Age lineages (2011); https://digital.csic.es/handle/10261/35427.

21. R. Risch, in *Überschuss ohne Staat-Politische Formen in der Vorgeschichte: 10. Mitteldeutscher Archäologentag vom 19. bis 21. Oktober 2017 in Halle (Saale)* (Landesmuseum für Vorgeschichte, 2018), pp. 45–65.

22. I. Mathieson, I. Lazaridis, N. Rohland, S. Mallick, N. Patterson, S. A. Roodenberg, E. Harney, K. Stewardson, D. Fernandes, M. Novak, K. Sirak, C. Gamba, E. R. Jones, B. Llamas, S. Dryomov, J. Pickrell, J. L. Arsuaga, J. M. B. de Castro, E. Carbonell, F. Gerritsen, A. Khokhlov, P. Kuznetsov, M. Lozano, H. Meller, O. Mochalov, V. Moiseyev, M. A. R. Guerra, J. Roodenberg, J. M. Vergès, J. Krause, A. Cooper, K. W. Alt, D. Brown, D. Anthony, C. Lalueza-Fox, W. Haak, R. Pinhasi, D. Reich, Genome-wide patterns of selection in 230 ancient Eurasians. *Nature* **528**, 499–503 (2015).

23. I. Lazaridis, D. Nadel, G. Rollefson, D. C. Merrett, N. Rohland, S. Mallick, D. Fernandes, M. Novak, B. Gamarra, K. Sirak, S. Connell, K. Stewardson, E. Harney, Q. Fu, G. Gonzalez-Fortes, E. R. Jones, S. A. Roodenberg, G. Lengyel, F. Bocquentin, B. Gasparian, J. M. Monge, M. Gregg, V. Eshed, A.-S. Mizrahi, C. Meiklejohn, F. Gerritsen, L. Bejenaru, M. Blüher, A. Campbell, G. Cavalleri, D. Comas, P. Froguel, E. Gilbert, S. M. Kerr, P. Kovacs, J. Krause, D. McGettigan, M. Merrigan, D. A. Merriwether, S. O'Reilly, M. B. Richards, O. Semino, M. Shamoon-Pour, G. Stefanescu, M. Stumvoll, A. Tönjes, A. Torroni, J. F. Wilson, L. Yengo, N. A. Hovhannisyan, N. Patterson, R. Pinhasi, D. Reich, Genomic insights into the origin of farming in the ancient Near East. *Nature* **536**, 419–424 (2016).

24. M. Lipson, A. Szécsényi-Nagy, S. Mallick, A. Pósa, B. Stégmár, V. Keerl, N. Rohland, K. Stewardson, M. Ferry, M. Michel, J. Oppenheimer, N. Broomandkhoshbacht, E. Harney, S. Nordenfelt, B. Llamas, B. Gusztáv Mende, K. Köhler, K. Oross, M. Bondár, T. Marton, A. Osztás, J. Jakucs, T. Paluch, F. Horváth, P. Csengeri, J. Koós, K. Sebők, A. Anders, P. Raczky, J. Regenye, J. P. Barna, S. Fábián, G. Serlegi, Z. Toldi, E. Gyöngyvér Nagy, J. Dani, E. Molnár, G. Pálfi, L. Márk, B. Melegh, Z. Bánfai, L. Domboróczki, J. Fernández-Eraso, J. Antonio Mujika-Alustiza, C. Alonso Fernández, J. Jiménez Echevarría, R. Bollongino, J. Orschiedt, K. Schierhold, H. Meller, A. Cooper, J. Burger, E. Bánffy, K. W. Alt, C. Lalueza-Fox, W. Haak, D. Reich, Parallel palaeogenomic transects reveal complex genetic history of early European farmers. *Nature* **551**, 368–372 (2017).

25. R. Martiniano, L. M. Cassidy, R. Ó'Maoldúin, R. McLaughlin, N. M. Silva, L. Manco, D. Fidalgo, T. Pereira, M. J. Coelho, M. Serra, J. Burger, R. Parreira, E. Moran, A. C. Valera, E. Porfirio, R. Boaventura, A. M. Silva, D. G. Bradley, The population genomics of archaeological transition in west Iberia: Investigation of ancient substructure using imputation and haplotype-based methods. *PLOS Genet.* **13**, e1006852 (2017).

26. C. Valdiosera, T. Günther, J. C. Vera-Rodríguez, I. Ureña, E. Iriarte, R. Rodríguez-Varela, L. G. Simões, R. M. Martínez-Sánchez, E. M. Svensson, H. Malmström, L. Rodríguez, J.-M. Bermúdez de Castro, E. Carbonell, A. Alday, J. A. Hernández Vera, A. Götherström, J.-M. Carretero, J. L. Arsuaga, C. I. Smith, M. Jakobsson, Four millennia of Iberian biomolecular prehistory illustrate the impact of prehistoric migrations at the far end of Eurasia. *Proc. Natl. Acad. Sci. U.S.A.* **115**, 3428–3433 (2018).

27. S. Brace, Y. Diekmann, T. J. Booth, L. van Dorp, Z. Faltyskova, N. Rohland, S. Mallick, I. Olalde, M. Ferry, M. Michel, J. Oppenheimer, N. Broomandkhoshbacht, K. Stewardson, R. Martiniano, S. Walsh, M. Kayser, S. Charlton, G. Hellenthal, I. Armit, R. Schulting, O. E. Craig, A. Sheridan, M. Parker Pearson, C. Stringer, D. Reich, M. G. Thomas, I. Barnes, Ancient genomes indicate population replacement in Early Neolithic Britain. *Nat. Ecol. Evol.* **3**, 765–771 (2019).

28. F. Molina González, J. A. Cámara Serrano, J. Capel Martínez, T. Nájera Colino, L. Sáez Pérez, Los Millares y la periodización de la Prehistoria Reciente del Sudeste, in *II - III Simposios de Prehistoria Cueva de Nerja* (Fundación Cueva de Nerja, Nerja, 2004), pp. 142–158.

29. A. C. Valera, Social change in the late 3rd millennium BC in Portugal: The twilight of enclosures, in *2200 BC—A Climatic Breakdown as a Cause for the Collapse of the Old World?*, H. Meller, R. Risch, R. Jung, H. W. Arz, Eds. (Landesmuseum für vorgeschichte, 2015), pp. 409–427.

30. V. Lull, *La" cultura" de El Argar: Un modelo para el estudio de las formaciones económico-sociales prehistóricas* (Ediciones Akal, 1983).

31. V. Lull, R. Micó, C. Rihuete Herrada, R. Risch, in *Sozialarchäologische Perspektiven: Gesellschaftlicher Wandel 5000–1500 v. Chr. Zwischen Atlantik und Kaukasus*, S. Hansen, J. Müller, Eds. (Archäologie in Eurasien, 2011), vol. 24, pp. 381–414.

32. V. Lull, R. Micó, C. Rihuete-Herrada, R. Risch, The La Bastida fortification: New light and new questions on Early Bronze Age societies in the western Mediterranean. *Antiquity* **88**, 395–410 (2014).

33. H. Schubart, *Mediterrane Beziehungen der El Argar-Kultur. Madrider Mitteilungen* **14**, 41–59 (1973).

34. V. Lull, R. Micó, C. Rihuete-Herrada, R. Risch, N. Escanilla, in *Actas del Congreso de Cronometrías Para la Historia de la Península Ibérica* (CEUR Workshop Proceedings 2024), J. A. Barceló, I. Bogdanovic. B. Morell, Eds. (IberCrono, Barcelona, 2017), pp. 143–162.

35. R. Risch, *Recursos naturales, medios de producción y explotación social. Un análisis económico de la industria lítica de Fuente Álamo (Almería), 2250-1400 ANE.* (P. von Zabern. Mainz, 2002).

36. V. Lull, R. M. Pérez, C. R. Herrada, R. Risch, Property relations in the Bronze Age of South-western Europe: An archaeological analysis of infant burials from El Argar (Almeria, Spain). *Proc. Prehist. Soc.* **71**, 247–268 (2005).

37. V. Lull, J. Estévez. Propuesta metodológica para el estudio de las necrópolis argáricas, in *Homenaje a Luis Siret (1934–1984), Consejería de Cultura de la Junta de Andalucía* (Dirección General de Bellas Artes, 1986), pp. 441–452.

38. V. Lull, R. Micó, C. Rihuete-Herrada, R. Risch, Funerary practices and kinship in an Early Bronze Age society: A Bayesian approach applied to the radiocarbon dating of Argaric double tombs. *J. Archaeol. Sci.* **40**, 4626–4634 (2013).

39. N. Rohland, E. Harney, S. Mallick, S. Nordenfelt, D. Reich, Partial uracil–DNA–glycosylase treatment for screening of ancient DNA. *Philos. Trans. R. Soc. Lond. B Biol. Sci.* **370**, 20130624 (2015).

40. T. Maricic, M. Whitten, S. Pääbo, Multiplexed DNA sequence capture of mitochondrial genomes using PCR products. *PLOS ONE* **5**, e14004 (2010).

41. Q. Fu, M. Hajdinjak, O. T. Moldovan, S. Constantin, S. Mallick, P. Skoglund, N. Patterson, N. Rohland, I. Lazaridis, B. Nickel, B. Viola, K. Prüfer, M. Meyer, J. Kelso, D. Reich, S. Pääbo, An early modern human from Romania with a recent Neanderthal ancestor. *Nature* **524**, 216–219 (2015).

42. A. B. Rohrlach, L. Papac, A. Childebayeva, M. Rivollat, V. Villalba-Mouco, G.U. Neumann, S. Penske, E. Skourtanioti, M. van de Loosdrecht, M. Akar, K. Boyadzhiev, Y. Boyadzhiev, M.-F. Deguilloux, M. Dobeš, Y.S. Erdal, M. Ernée, M. Frangipane, M. Furmanek, S. Friederich, E. Ghesquière, A. Haluszko, S. Hansen, M. Küßner, M. Mannino, R. Özbal, S. Reinhold, S. Rottier, D. C. Salazar-García, J. Soler Diaz, P.W. Stockhammer, C. Roca de Togores Muñoz, K. Aslihan Yener, C. Posth, J. Krause, A. Herbig, W. Haak, Using Y-chromosome capture enrichment to resolve haplogroup H2 shows new evidence for a two-Path Neolithic expansion to Western Europe. *Sci. Rep.* **11**, 15005 (2021).

43. A. Peltzer, G. Jäger, A. Herbig, A. Seitz, C. Kniep, J. Krause, K. Nieselt, EAGER: Efficient ancient genome reconstruction. *Genome Biol.* **17**, 60 (2016).

44. T. S. Korneliussen, A. Albrechtsen, R. Nielsen, ANGSD: Analysis of next generation sequencing data. *BMC Bioinformatics* **15**, 356 (2014).

45. Q. Fu, A. Mittnik, P. L. F. Johnson, K. Bos, M. Lari, R. Bollongino, C. Sun, L. Giemsch, R. Schmitz, J. Burger, A. M. Ronchitelli, F. Martini, R. G. Cremonesi, J. Svoboda, P. Bauer, D. Caramelli, S. Castellano, D. Reich, S. Pääbo, J. Krause, A revised timescale for human evolution based on ancient mitochondrial genomes. *Curr. Biol.* **23**, 553–559 (2013).

46. A. Mittnik, C.-C. Wang, J. Svoboda, J. Krause, A molecular approach to the sexing of the triple burial at the upper paleolithic site of Dolní Věstonice. *PLOS ONE* **11**, e0163019 (2016).

47. M. Lipatov, K. Sanjeev, R. Patro, K. R. Veeramah, Maximum likelihood estimation of biological relatedness from low coverage sequencing data. bioRxiv 023374 [**Preprint**]. 29 July 2015. https://doi.org/10.1101/023374.

48. D. J. Kennett, S. Plog, R. J. George, B. J. Culleton, A. S. Watson, P. Skoglund, N. Rohland, S. Mallick, K. Stewardson, L. Kistler, S. A. LeBlanc, P. M. Whiteley, D. Reich, G. H. Perry, Archaeogenomic evidence reveals prehistoric matrilineal dynasty. *Nat. Commun.* **8**, 14115 (2017).

49. J. M. Monroy Kuhn, M. Jakobsson, T. Günther, Estimating genetic kin relationships in prehistoric populations. *PLOS ONE* **13**, e0195491 (2018).

50. M. L. Antonio, Z. Gao, H. M. Moots, M. Lucci, F. Candilio, S. Sawyer, V. Oberreiter, D. Calderon, K. Devitofranceschi, R. C. Aikens, S. Aneli, F. Bartoli, A. Bedini, O. Cheronet, D. J. Cotter, D. M. Fernandes, G. Gasperetti, R. Grifoni, A. Guidi, F. La Pastina, E. Loreti, D. Manacorda, G. Matullo, S. Morretta, A. Nava, V. Fiocchi Nicolai, F. Nomi, C. Pavolini, M. Pentiricci, P. Pergola, M. Piranomonte, R. Schmidt, G. Spinola, A. Sperduti, M. Rubini, L. Bondioli, A. Coppa, R. Pinhasi, J. K. Pritchard, Ancient Rome: A genetic crossroads of Europe and the Mediterranean. *Science* **366**, 708–714 (2019).

51. D. M. Fernandes, A. Mittnik, I. Olalde, I. Lazaridis, O. Cheronet, N. Rohland, S. Mallick, R. Bernardos, N. Broomandkhoshbacht, J. Carlsson, B. J. Culleton, M. Ferry, B. Gamarra, M. Lari, M. Mah, M. Michel, A. Modi, M. Novak, J. Oppenheimer, K. A. Sirak, K. Stewardson, K. Mandl, C. Schattke, K. T. Özdoğan, M. Lucci, G. Gasperetti, F. Candilio, G. Salis, S. Vai, E. Camarós, C. Calò, G. Catalano, M. Cueto, V. Forgia, M. Lozano, E. Marini, M. Micheletti, R. M. Miccichè, M. R. Palombo, D. Ramis, V. Schimmenti, P. Sureda, L. Teira, M. Teschler-Nicola, D. J. Kennett, C. Lalueza-Fox, N. Patterson, L. Sineo, A. Coppa, D. Caramelli, R. Pinhasi, D. Reich, The spread of steppe and Iranian-related ancestry in the islands of the western Mediterranean. *Nat. Ecol. Evol.* **4**, 334–345 (2020).

52. J. H. Marcus, C. Posth, H. Ringbauer, L. Lai, R. Skeates, C. Sidore, J. Beckett, A. Furtwängler, A. Olivieri, C. W. K. Chiang, H. Al-Asadi, K. Dey, T. A. Joseph, C.-C. Liu, C. Der Sarkissian, R. Radzevičiūtė, M. Michel, M. G. Gradoli, P. Marongiu, S. Rubino, V. Mazzarello, D. Rovina, A. La Fragola, R. M. Serra, P. Bandiera, R. Bianucci, E. Pompianu, C. Murgia, M. Guirguis, R. P. Orquin,

N. Tuross, P. van Dommelen, W. Haak, D. Reich, D. Schlessinger, F. Cucca, J. Krause, J. Novembre, Genetic history from the Middle Neolithic to present on the Mediterranean island of Sardinia. *Nat. Commun.* **11**, 939 (2020).

53. E. Skourtanioti, Y. S. Erdal, M. Frangipane, F. Balossi Restelli, K. A. Yener, F. Pinnock, P. Matthiae, R. Özbal, U.-D. Schoop, F. Guliyev, T. Akhundov, B. Lyonnet, E. L. Hammer, S. E. Nugent, M. Burri, G. U. Neumann, S. Penske, T. Ingman, M. Akar, R. Shafiq, G. Palumbi, S. Eisenmann, M. D'Andrea, A. B. Rohrlach, C. Warinner, C. Jeong, P. W. Stockhammer, W. Haak, J. Krause, Genomic history of Neolithic to Bronze Age Anatolia, Northern Levant, and Southern Caucasus. *Cell* **181**, 1158–1175.e28 (2020).

54. N. Patterson, P. Moorjani, Y. Luo, S. Mallick, N. Rohland, Y. Zhan, T. Genschoreck, T. Webster, D. Reich, Ancient admixture in human history. *Genetics* **192**, 1065–1093 (2012).

55. V. Heyd, Kossinna's smile. *Antiquity* **91**, 348–359 (2017).

56. Q. Fu, C. Posth, M. Hajdinjak, M. Petr, S. Mallick, D. Fernandes, A. Furtwängler, W. Haak, M. Meyer, A. Mittnik, B. Nickel, A. Peltzer, N. Rohland, V. Slon, S. Talamo, I. Lazaridis, M. Lipson, I. Mathieson, S. Schiffels, P. Skoglund, A. P. Derevianko, N. Drozdov, V. Slavinsky, A. Tsybankov, R. G. Cremonesi, F. Mallegni, B. Gély, E. Vacca, M. R. G. Morales, L. G. Straus, C. Neugebauer-Maresch, M. Teschler-Nicola, S. Constantin, O. T. Moldovan, S. Benazzi, M. Peresani, D. Coppola, M. Lari, S. Ricci, A. Ronchitelli, F. Valentin, C. Thevenet, K. Wehrberger, D. Grigorescu, H. Rougier, I. Crevecoeur, D. Flas, P. Semal, M. A. Mannino, C. Cupillard, H. Bocherens, N. J. Conard, K. Harvati, V. Moiseyev, D. G. Drucker, J. Svoboda, M. P. Richards, D. Caramelli, R. Pinhasi, J. Kelso, N. Patterson, J. Krause, S. Pääbo, D. Reich, The genetic history of Ice Age Europe. *Nature* **534**, 200–205 (2016).

57. V. Villalba-Mouco, M. S. van de Loosdrecht, C. Posth, R. Mora, J. Martínez-Moreno, M. Rojo-Guerra, D. C. Salazar-García, J. I. Royo-Guillén, M. Kunst, H. Rougier, I. Crevecoeur, H. Arcusa-Magallón, C. Tejedor-Rodríguez, I. García-Martínez de Lagrán, R. Garrido-Pena, K. W. Alt, C. Jeong, S. Schiffels, P. Utrilla, J. Krause, W. Haak, Survival of Late Pleistocene hunter-gatherer ancestry in the Iberian peninsula. *Curr. Biol.* **29**, 1169–1177.e7 (2019).

58. M. Rivollat, C. Jeong, S. Schiffels, İ. Küçükkalıpçı, M.-H. Pemonge, A. B. Rohrlach, K. W. Alt, D. Binder, S. Friederich, E. Ghesquière, D. Gronenborn, L. Laporte, P. Lefranc, H. Meller, H. Réveillas, E. Rosenstock, S. Rottier, C. Scarre, L. Soler, J. Wahl, J. Krause, M.-F. Deguilloux, W. Haak, Ancient genome-wide DNA from France highlights the complexity of interactions between Mesolithic hunter-gatherers and Neolithic farmers. *Sci. Adv.* **6**, eaaz5344 (2020).

59. M. S. van de Loosdrecht, M. A. Mannino, S. Talamo, V. Villalba-Mouco, C. Posth, F. Aron, G. Brandt, M. Burri, C. Freund, R. Radzeviciute, R. Stahl, A. Wissgott, L. Klausnitzer, S. Nagel, M. Meyer, A. Tagliacozzo, M. Piperno, S. Tusa, *C. Collina*, V. Schimmenti, R. D. Salvo, K. Prüfer, J.-J. Hublin, S. Schiffels, C. Jeong, W. Haak, J. Krause, Genomic and dietary transitions during the Mesolithic and Early Neolithic in Sicily. bioRxiv 2020.03.11.986158 [**Preprint**]. 12 March 2020. https://doi.org/10.1101/2020.03.11.986158.

60. D. H. Alexander, J. Novembre, K. Lange, Fast model-based estimation of ancestry in unrelated individuals. *Genome Res.* **19**, 1655–1664 (2009).

61. J. A. Alcover, The first Mallorcans: Prehistoric colonization in the Western Mediterranean. *J. World Prehist.* **21**, 19–84 (2008).

62. R. Micó, Radiocarbon dating and Balearic prehistory: Reviewing the periodization of the prehistoric sequence. *Radiocarbon* **48**, 421–434 (2006).

63. L. García Sanjuán, J. M. Vargas Jiménez, L. M. Cáceres Puro, M. E. Costa Caramé, M. Díaz-Guardamino Uribe, M. Díaz-Zorita Bonilla, Á. Fernández Flores, V. Hurtado Pérez, P. M. López Aldana, E. Méndez Izquierdo, A. Pajuelo Pando, J. Rodríguez Vidal, D. Wheatley, C. Bronk Ramsey, A. Delgado-Huertas, E. Dunbar, A. Mora González, A. Bayliss, N. Beavan, D. Hamilton, A. Whittle, Assembling the dead, gathering the living: Radiocarbon dating and Bayesian modelling for Copper Age Valencina de la Concepción (Seville, Spain). *J. World Prehist.* **31**, 179–313 (2018).

64. G. Aranda Jiménez, M. Díaz-Zorita Bonilla, D. Hamilton, L. Milesi, M. Sánchez Romero, The radiocarbon chronology and temporality of the megalithic cemetery of Los Millares (Almería, Spain). *Archaeol. Anthropol. Sci.* **12**, 104 (2020).

65. A. C. Valera, Social change in the late 3rd millennium BC in Portugal: The twilight of enclosures, in *2200 BC: A Climatic Break-down as a Cause for the Collapse of the Old World*, H. Meller, H. Arz, R. Jung, R. Risch, Eds. (Landesmuseum für Vorgeschichte, Halle, 2014), pp. 409–428.

66. A. Blanco-González, K. T. Lillios, J. A. López-Sáez, B. L. Drake, Cultural, demographic and environmental dynamics of the Copper and Early Bronze Age in Iberia (3300–1500 BC): Towards an interregional multiproxy comparison at the time of the 4.2 ky BP event. *J. World Prehist.* **31**, 1–79 (2018).

67. M. Hinz, J. Schirrmacher, J. Kneisel, C. Rinne, M. Weinelt, The Chalcolithic–Bronze Age transition in southern Iberia under the influence of the 4.2 kyr event? A correlation of climatological and demographic proxies. *J. Neolithic Archaeol.* **21**, 1–26 (2019).

68. J. Schirrmacher, J. Kneisel, D. Knitter, W. Hamer, M. Hinz, R. R. Schneider, M. Weinelt, Spatial patterns of temperature, precipitation, and settlement dynamics on the Iberian Peninsula during the Chalcolithic and the Bronze Age. *Quat. Sci. Rev.* **233**, 106220 (2020).

69. K. T. Lillios, A. Blanco-González, B. L. Drake, J. A. López-Sáez, Mid-late Holocene climate, demography, and cultural dynamics in Iberia: A multi-proxy approach. *Quat. Sci. Rev.* **135**, 138–153 (2016).

0. V. Lull, R. Micó, C. Rihuete, R. Risch, in *The Matter of Prehistory. Papers in Honour of Antonio Gilman Guillén*, P. D. del Río, K. Lillios, I. Sastre, Eds. (Biblioteca Praehistorica Hispana, 36—Consejo Superior de Investigaciones Científicas, 2020), pp. 191–209.

71. I. Lazaridis, A. Mittnik, N. Patterson, S. Mallick, N. Rohland, S. Pfrengle, A. Furtwängler, A. Peltzer, C. Posth, A. Vasilakis, P. J. P. McGeorge, E. Konsolaki-Yannopoulou, G. Korres, H. Martlew, M. Michalodimitrakis, M. Özsait, N. Özsait, A. Papathanasiou, M. Richards, S. A.

Roodenberg, Y. Tzedakis, R. Arnott, D. M. Fernandes, J. R. Hughey, D. M. Lotakis, P. A. Navas, Y. Maniatis, J. A. Stamatoyannopoulos, K. Stewardson, P. Stockhammer, R. Pinhasi, D. Reich, J. Krause, G. Stamatoyannopoulos, Genetic origins of the Minoans and Mycenaeans. *Nature* **548**, 214–218 (2017).

72. E. R. Jones, G. Gonzalez-Fortes, S. Connell, V. Siska, A. Eriksson, R. Martiniano, R. L. McLaughlin, M. Gallego Llorente, L. M. Cassidy, C. Gamba, T. Meshveliani, O. Bar-Yosef, W. Müller, A. Belfer-Cohen, Z. Matskevich, N. Jakeli, T. F. G. Higham, M. Currat, D. Lordkipanidze, M. Hofreiter, A. Manica, R. Pinhasi, D. G. Bradley, Upper Palaeolithic genomes reveal deep roots of modern Eurasians. *Nat. Commun.* **6**, 8912 (2015).

73. H. Ringbauer, J. Novembre, M. Steinrücken, Parental relatedness through time revealed by runs of homozygosity in ancient DNA. *Nat. Commun.* **12**, 5425 (2021).

74. H. Ringbauer, M. Steinrücken, L. Fehren-Schmitz, D. Reich, Increased rate of close-kin unions in the central Andes in the half millennium before European contact. *Curr. Biol.* **30**, R980–R981 (2020).

75. A. Goldberg, N. A. Rosenberg, Beyond 2/3 and 1/3: The complex signatures of sex-biased admixture on the X chromosome. *Genetics* **201**, 263–279 (2015).

76. I. Mathieson, S. Alpaslan-Roodenberg, C. Posth, A. Szécsényi-Nagy, N. Rohland, S. Mallick, I. Olalde, N. Broomandkhoshbacht, F. Candilio, O. Cheronet, D. Fernandes, M. Ferry, B. Gamarra, G. G. Fortes, W. Haak, E. Harney, E. Jones, D. Keating, B. Krause-Kyora, I. Kucukkalipci, M. Michel, A. Mittnik, K. Nägele, M. Novak, J. Oppenheimer, N. Patterson, S. Pfrengle, K. Sirak, K. Stewardson, S. Vai, S. Alexandrov, K. W. Alt, R. Andreescu, D. Antonović, A. Ash, N. Atanassova, K. Bacvarov, M. B. Gusztáv, H. Bocherens, M. Bolus, A. Boroneanţ, Y. Boyadzhiev, A. Budnik, J. Burmaz, S. Chohadzhiev, N. J. Conard, R. Cottiaux, M. Čuka, C. Cupillard, D. G. Drucker, N. Elenski, M. Francken, B. Galabova, G. Ganetsovski, B. Gély, T. Hajdu, V. Handzhyiska, K. Harvati, T. Higham, S. Iliev, I. Janković, I. Karavanić, D. J. Kennett, D. Komšo, A. Kozak, D. Labuda, M. Lari, C. Lazar, M. Leppek, K. Leshtakov, D. L. Vetro, D. Los, I. Lozanov, M. Malina, F. Martini, K. McSweeney, H. Meller, M. Menđušić, P. Mirea, V. Moiseyev, V. Petrova, T. D. Price, A. Simalcsik, L. Sineo, M. Šlaus, V. Slavchev, P. Stanev, A. Starović, T. Szeniczey, S. Talamo, M. Teschler-Nicola, C. Thevenet, I. Valchev, F. Valentin, S. Vasilyev, F. Veljanovska, S. Venelinova, E. Veselovskaya, B. Viola, C. Virag, J. Zaninović, S. Zäuner, P. W. Stockhammer, G. Catalano, R. Krauß, D. Caramelli, G. Zariņa, B. Gaydarska, M. Lillie, A. G. Nikitin, I. Potekhina, A. Papathanasiou, D. Borić, C. Bonsall, J. Krause, R. Pinhasi, D. Reich, The genomic history of southeastern Europe. *Nature* **555**, 197–203 (2018).

77. A. Mittnik, K. Massy, C. Knipper, F. Wittenborn, R. Friedrich, S. Pfrengle, M. Burri, N. Carlichi-Witjes, H. Deeg, A. Furtwängler, M. Harbeck, K. von Heyking, C. Kociumaka, I. Kucukkalipci, S. Lindauer, S. Metz, A. Staskiewicz, A. Thiel, J. Wahl, W. Haak, E. Pernicka, S. Schiffels, P. W. Stockhammer, J. Krause, Kinship-based social inequality in Bronze Age Europe. *Science* **366**, 731–734 (2019).

78. J. Dabney, M. Knapp, I. Glocke, M.-T. Gansauge, A. Weihmann, B. Nickel, C. Valdiosera, N. García, S. Pääbo, J.-L. Arsuaga, M. Meyer, Complete mitochondrial genome sequence of a Middle Pleistocene cave bear reconstructed from ultrashort DNA fragments. *Proc. Natl. Acad. Sci. U.S.A.* **110**, 15758–15763 (2013).

79. M. Kircher, S. Sawyer, M. Meyer, Double indexing overcomes inaccuracies in multiplex sequencing on the Illumina platform. *Nucleic Acids Res.* **40**, e3 (2012).

80. M. Meyer, M. Kircher, Illumina sequencing library preparation for highly multiplexed target capture and sequencing. *Cold Spring Harb. Protoc.* **2010** , pdb.prot5448 (2010).

81. M. Schubert, S. Lindgreen, L. Orlando, AdapterRemoval v2: Rapid adapter trimming, identification, and read merging. *BMC Res. Notes* **9**, 88 (2016).

82. H. Li, R. Durbin, Fast and accurate short read alignment with Burrows–Wheeler transform. *Bioinformatics* **25**, 1754–1760 (2009).

83. A. Ginolhac, H. Jónsson, L. Orlando, M. Schubert, P. L. F. Johnson, mapDamage2.0: Fast approximate Bayesian estimates of ancient DNA damage parameters. *Bioinformatics* **29**, 1682–1684 (2013).

84. M. Kearse, R. Moir, A. Wilson, S. Stones-Havas, M. Cheung, S. Sturrock, S. Buxton, A. Cooper, S. Markowitz, C. Duran, T. Thierer, B. Ashton, P. Meintjes, A. Drummond, Geneious Basic: An integrated and extendable desktop software platform for the organization and analysis of sequence data. *Bioinformatics* **28**, 1647–1649 (2012).

85. H. Li, B. Handsaker, A. Wysoker, T. Fennell, J. Ruan, N. Homer, G. Marth, G. Abecasis, R. Durbin; 1000 Genome Project Data Processing Subgroup, The sequence alignment/Map format and SAMtools. *Bioinformatics* **25**, 2078–2079 (2009).

86. H. Weissensteiner, D. Pacher, A. Kloss-Brandstätter, L. Forer, G. Specht, H.-J. Bandelt, F. Kronenberg, A. Salas, S. Schönherr, HaploGrep 2: Mitochondrial haplogroup classification in the era of high-throughput sequencing. *Nucleic Acids Res.* **44**, W58–W63 (2016).

87. M. van de Loosdrecht, A. Bouzouggar, L. Humphrey, C. Posth, N. Barton, A. Aximu-Petri, B. Nickel, S. Nagel, E. H. Talbi, M. A. El Hajraoui, S. Amzazi, J.-J. Hublin, S. Pääbo, S. Schiffels, M. Meyer, W. Haak, C. Jeong, J. Krause, Pleistocene North African genomes link Near Eastern and sub-Saharan African human populations. *Science* **360**, 548–552 (2018).

88. C. C. Cockerham, Higher order probability functions of identity of allelles by descent. *Genetics* **69**, 235–246 (1971).

89. S. Walsh, F. Liu, A. Wollstein, L. Kovatsi, A. Ralf, A. Kosiniak-Kamysz, W. Branicki, M. Kayser, The HIrisPlex system for simultaneous prediction of hair and eye colour from DNA. *Forensic Sci. Int. Genet.* **7**, 98–115 (2013).

90. N. Patterson, A. L. Price, D. Reich, Population structure and eigenanalysis. *PLOS Genet.* **2**, e190 (2006).

91. C.-C. Wang, S. Reinhold, A. Kalmykov, A. Wissgott, G. Brandt, C. Jeong, O. Cheronet, M. Ferry, E. Harney, D. Keating, S. Mallick, N. Rohland, K. Stewardson, A. R. Kantorovich, V. E. Maslov, V. G. Petrenko, V. R. Erlikh, B. C. Atabiev, R. G. Magomedov, P. L. Kohl, K. W. Alt, S. L. Pichler, C. Gerling, H. Meller, B. Vardanyan, L. Yeganyan, A. D. Rezepkin, D. Mariaschk, N. Berezina, J. Gresky, K. Fuchs, C. Knipper, S. Schiffels, E. Balanovska, O. Balanovsky, I. Mathieson, T. Higham, Y. B. Berezin, A. Buzhilova, V. Trifonov, R. Pinhasi, A. B. Belinskij, D. Reich, S. Hansen, J. Krause, W. Haak, Ancient human genome-wide data from a 3000-year interval in the Caucasus corresponds with eco-geographic regions. *Nat. Commun.* **10**, 590 (2019).

92. S. Purcell, B. Neale, K. Todd-Brown, L. Thomas, M. A. R. Ferreira, D. Bender, J. Maller, P. Sklar, P. I. W. de Bakker, M. J. Daly, P. C. Sham, PLINK: A tool set for whole-genome association and population-based linkage analyses. *Am. J. Hum. Genet.* **81**, 559–575 (2007).

93. P. Moorjani, S. Sankararaman, Q. Fu, M. Przeworski, N. Patterson, D. Reich, A genetic method for dating ancient genomes provides a direct estimate of human generation interval in the last 45,000 years. *Proc. Natl. Acad. Sci. U.S.A.* **113**, 5652–5657 (2016).

94. V. Lull, C. Rihuete Herrada, R. Risch, E. Celdrán Beltrán, M. I. Fregeiro Morador, C. Oliart Caravatti, C. Velasco Felipe, *La Almoloya (Pliego-Murcia): Murcia: Integral, Sociedad Para el Desarrollo Rural* (Integral - Sociedad para el Desarrollo Rural, Bullas, Spain, 2015).

95. V. Lull, C. Rihuete Herrada, R. Risch, B. Bonora, E. Celdrán Beltrán, M. I. Fregeiro Morador, C. Molero, C. Moreno, C. Oliart Caravatti, C. Velasco-Felipe, L. Andúgar, W. Haak, V. Villalba-Mouco, R. Micó, Emblems and spaces of power during the Argaric Bronze Age at La Almoloya, Murcia. *Antiquity* **95**, 329–348 (2021).

96. V. Lull, R. Micó, C. Rihuete Herrada, R. Risch, *La Bastida y Tira del Lienzo (Totana-Murcia): Murcia: Integral, Sociedad Para el Desarrollo Rural* (Integral - Sociedad para el Desarrollo Rural, Bullas, Spain, 2015).

97. C. Knipper, C. Rihuete-Herrada, J. Voltas, P. Held, V. Lull, R. Micó, R. Risch, K. W. Alt, Reconstructing Bronze Age diets and farming strategies at the early Bronze Age sites of La Bastida and Gatas (southeast Iberia) using stable isotope analysis. *PLOS ONE* **15**, e0229398 (2020).

98. A. Szécsényi-Nagy, C. Roth, G. Brandt, C. Rihuete-Herrada, C. Tejedor-Rodríguez, P. Held, Í. García-Martínez-de-Lagrán, H. Arcusa Magallón, S. Zesch, C. Knipper, E. Bánffy, S. Friederich, H. Meller, P. Bueno Ramírez, R. Barroso Bermejo, R. de Balbín Behrmann, A. M. Herrero-Corral, R. Flores Fernández, C. Alonso Fernández, J. Jiménez Echevarria, L. Rindlisbacher, C. Oliart, M.-I. Fregeiro, I. Soriano, O. Vicente, R. Micó, V. Lull, J. Soler Díaz, J. A. López Padilla, C. Roca de Togores Muñoz, M. S. Hernández Pérez, F. J. Jover Maestre, J. Lomba Maurandi, A. Avilés Fernández, K. T. Lillios, A. M. Silva, M. Magalhães Ramalho, L. M. Oosterbeek, C. Cunha, A. J. Waterman, J. Roig Buxó, A. Martínez, J. Ponce Martínez, M. Hunt Ortiz, J. C. Mejías-García, J. C. Pecero Espín, R. Cruz-Auñón Briones, T. Tomé, E. Carmona Ballestero, J. L. Cardoso, A. C. Araújo, C. Liesau von Lettow-Vorbeck, C. Blasco Bosqued, P. Ríos Mendoza, A. Pujante, J. I. Royo-Guillén, M. A. Esquembre Beviá, V. M. Dos Santos Goncalves, R. Parreira, E. Morán Hernández, E. Méndez Izquierdo, J. Vega y Miguel, R. Menduiña García, V. Martínez Calvo, O.

López Jiménez, J. Krause, S. L. Pichler, R. Garrido-Pena, M. Kunst, R. Risch, M. A. Rojo-Guerra, W. Haak, K. W. Alt, The maternal genetic make-up of the Iberian Peninsula between the Neolithic and the Early Bronze Age. *Sci. Rep.* **7**, 15644 (2017).

99. J. A. Soler Díaz, C. Roca de Togores, Ritual funerario en la Cova d'En Pardo ca. 3.350–2.850 CAL ANE: Espacialidad, cronología y territorio cultural, in *Cova d'En Pardo: Arqueología en la Memoria: Excavaciones de M. Tarradell, V. Pascual y E. Llobregat (1961–1965), Catálogo de Materiales del Museo de Alcoy y Estudios a Partir de las Campañas del MARQ (1993–2007) en la Cavidad de Planes,* Alicante. (Museo Arqueológico de Alicante—MARQ, 2012), pp. 205–248.

100. J. A. S. Díaz, C. Roca de Togores Muñoz, Estudio de los restos humanos encontrados en las intervenciones practicadas en los años 1961 y 1965 en la Cova d'En Pardo, Planes, Alicante: análisis antropológico y aproximación a su contexto cultural. *Saguntum* Extra 2 (1999), pp. 369–377.

101. C. Roca de Togores Muñoz, J. A. S. Díaz, Restos humanos en la Cova d'en Pardo (Planes). Problemática y avance de resultados de la investigación antropológica en una cavidad de inhumación múltiple excavada en dos etapas: 1961-1965 y 1993-2007, in *Cova d'En Pardo: Arqueología en la Memoria: Excavaciones de M. Tarradell, V. Pascual y E. Llobregat (1961–1965), Catálogo de Materiales del Museo de Alcoy y Estudios a Partir de las Campañas del MARQ (1993–2007) en la Cavidad de Planes, Alicante* (Museo Arqueológico de Alicante—MARQ, 2012), pp. 193–204.

102. V. Lull, R. Micó, C. Rihuete, R. Risch, *La Cova des Càrritx y la Cova des Mussol. Ideología y Sociedad en la Prehistoria de de Menorca* (Consell Insular de Menorca, 1999).

103. M. De Cet, *Long-term Social Development on a Mediterranean Island: Menorca Between 1600 BCE and 1900 CE* (In Kommission bei Verlag Dr. Rudolf Habelt GmbH, 2017).

104. T. Günther, C. Valdiosera, H. Malmström, I. Ureña, R. Rodriguez-Varela, Ó. O. Sverrisdóttir, E. A. Daskalaki, P. Skoglund, T. Naidoo, E. M. Svensson, J. M. Bermúdez de Castro, E. Carbonell, M. Dunn, J. Storå, E. Iriarte, J. L. Arsuaga, J.-M. Carretero, A. Götherström, M. Jakobsson, Ancient genomes link early farmers from Atapuerca in Spain to modern-day Basques. *Proc. Natl. Acad. Sci. U.S.A.* **112**, 11917–11922 (2015).

105. P. de Barros Damgaard, N. Marchi, S. Rasmussen, M. Peyrot, G. Renaud, T. Korneliussen, J. V. Moreno-Mayar, M. W. Pedersen, A. Goldberg, E. Usmanova, N. Baimukhanov, V. Loman, L. Hedeager, A. G. Pedersen, K. Nielsen, G. Afanasiev, K. Akmatov, A. Aldashev, A. Alpaslan, G. Baimbetov, V. I. Bazaliiskii, A. Beisenov, B. Boldbaatar, B. Boldgiv, C. Dorzhu, S. Ellingvag, D. Erdenebaatar, R. Dajani, E. Dmitriev, V. Evdokimov, K. M. Frei, A. Gromov, A. Goryachev, H. Hakonarson, T. Hegay, Z. Khachatryan, R. Khaskhanov, E. Kitov, A. Kolbina, T. Kubatbek, A. Kukushkin, I. Kukushkin, N. Lau, A. Margaryan, I. Merkyte, I. V. Mertz, V. K. Mertz, E. Mijiddorj, V. Moiyesev, G. Mukhtarova, B. Nurmukhanbetov, Z. Orozbekova, I. Panyushkina, K. Pieta, V. Smrčka, I. Shevnina, A. Logvin, K.-G. Sjögren, T. Štolcová, A. M. Taravella, K. Tashbaeva, A. Tkachev, T. Tulegenov, D. Voyakin, L. Yepiskoposyan, S. Undrakhbold, V. Varfolomeev, A. Weber, M. A. Wilson Sayres, N. Kradin, M. E. Allentoft, L. Orlando, R. Nielsen,

M. Sikora, E. Heyer, K. Kristiansen, E. Willerslev, 137 ancient human genomes from across the Eurasian steppes. *Nature* **557**, 369–374 (2018).

106. A. Mittnik, C.-C. Wang, S. Pfrengle, M. Daubaras, G. Zariņa, F. Hallgren, R. Allmäe, V. Khartanovich, V. Moiseyev, M. Tõrv, A. Furtwängler, A. Andrades Valtueña, M. Feldman, C. Economou, M. Oinonen, A. Vasks, E. Balanovska, D. Reich, R. Jankauskas, W. Haak, S. Schiffels, J. Krause, The genetic prehistory of the Baltic Sea region. *Nat. Commun.* **9**, 442 (2018).

107. R. Rodríguez-Varela, T. Günther, M. Krzewińska, J. Storå, T. H. Gillingwater, M. MacCallum, J. L. Arsuaga, K. Dobney, C. Valdiosera, M. Jakobsson, A. Götherström, L. Girdland-Flink, Genomic analyses of pre-European conquest human remains from the Canary Islands reveal close affinity to modern North Africans. *Curr. Biol.* **28**, 1677–1679 (2018).

108. V. M. Narasimhan, N. Patterson, P. Moorjani, N. Rohland, R. Bernardos, S. Mallick, I. Lazaridis, N. Nakatsuka, I. Olalde, M. Lipson, A. M. Kim, L. M. Olivieri, A. Coppa, M. Vidale, J. Mallory, V. Moiseyev, E. Kitov, J. Monge, N. Adamski, N. Alex, N. Broomandkhoshbacht, F. Candilio, K. Callan, O. Cheronet, B. J. Culleton, M. Ferry, D. Fernandes, S. Freilich, B. Gamarra, D. Gaudio, M. Hajdinjak, É. Harney, T. K. Harper, D. Keating, A. M. Lawson, M. Mah, K. Mandl, M. Michel, M. Novak, J. Oppenheimer, N. Rai, K. Sirak, V. Slon, K. Stewardson, F. Zalzala, Z. Zhang, G. Akhatov, A. N. Bagashev, A. Bagnera, B. Baitanayev, J. Bendezu-Sarmiento, A. A. Bissembaev, G. L. Bonora, T. T. Chargynov, T. Chikisheva, P. K. Dashkovskiy, A. Derevianko, M. Dobeš, K. Douka, N. Dubova, M. N. Duisengali, D. Enshin, A. Epimakhov, A. V. Fribus, D. Fuller, A. Goryachev, A. Gromov, S. P. Grushin, B. Hanks, M. Judd, E. Kazizov, A. Khokhlov, A. P. Krygin, E. Kupriyanova, P. Kuznetsov, D. Luiselli, F. Maksudov, A. M. Mamedov, T. B. Mamirov, C. Meiklejohn, D. C. Merrett, R. Micheli, O. Mochalov, S. Mustafokulov, A. Nayak, D. Pettener, R. Potts, D. Razhev, M. Rykun, S. Sarno, T. M. Savenkova, K. Sikhymbaeva, S. M. Slepchenko, O. A. Soltobaev, N. Stepanova, S. Svyatko, K. Tabaldiev, M. Teschler-Nicola, A. A. Tishkin, V. V. Tkachev, S. Vasilyev, P. Velemínský, D. Voyakin, A. Yermolayeva, M. Zahir, V. S. Zubkov, A. Zubova, V. S. Shinde, C. Lalueza-Fox, M. Meyer, D. Anthony, N. Boivin, K. Thangaraj, D. J. Kennett, M. Frachetti, R. Pinhasi, D. Reich, The formation of human populations in South and Central Asia. *Science* **365**, eaat7487 (2019).

109. H. F. Klinefelter Jr, E. C. Reifenstein Jr, Syndrome characterized by gynecomastia, aspermatogenesis without A-Leydigism, and increased excretion of follicle-stimulating hormone. *J. Clin. Endocrinol.* 2, 615–627 (1942).

110. P. Jacobs, A. G. Baikie, T. N. MacGregor, N. Maclean, D. G. Harnden, Evidence for the existence of the human“ super female.” *Lancet* **274**, 423–425 (1959).

111. R. Boada, J. Janusz, C. Hutaff-Lee, N. Tartaglia, The cognitive phenotype in Klinefelter syndrome: A review of the literature including genetic and hormonal factors. *Dev. Disabil. Res. Rev.* **15**, 284–294 (2009).

112. S. S. Ebenesersdóttir, M. Sandoval-Velasco, E. D. Gunnarsdóttir, A. Jagadeesan, V. B. Guðmundsdóttir, E. L. Thordardóttir, M. S. Einarsdóttir, K. H. S. Moore, Á. Sigurðsson, D. N. Magnúsdóttir, H. Jónsson, S. Snorradóttir, E. Hovig, P. Møller, I. Kockum, T. Olsson, L.

Alfredsson, T. F. Hansen, T. Werge, G. L. Cavalleri, E. Gilbert, C. Lalueza-Fox, J. W. Walser III, S. Kristjánsdóttir, S. Gopalakrishnan, L. Árnadóttir, Ó. Þ. Magnússon, M. T. P. Gilbert, K. Stefánsson, A. Helgason, Ancient genomes from Iceland reveal the making of a human population. *Science* **360**, 1028–1032 (2018).

113. M. Otter, C. T. Schrander-Stumpel, L. M. G. Curfs, Triple X syndrome: A review of the literature. *Eur. J. Hum. Genet.* **18**, 265–271 (2010).

114. M. Rafique, S. AlObaid, D. Al-Jaroudi, 47, XXX syndrome with infertility, premature ovarian insufficiency, and streak ovaries. *Clin. Case Rep.* **7**, 1238–1241 (2019).

115. H. Schroeder, A. Margaryan, M. Szmyt, B. Theulot, P. Włodarczak, S. Rasmussen, S. Gopalakrishnan, A. Szczepanek, T. Konopka, T. Z. T. Jensen, B. Witkowska, S. Wilk, M. M. Przybyła, Ł. Pospieszny, K.-G. Sjögren, Z. Belka, J. Olsen, K. Kristiansen, E. Willerslev, K. M. Frei, M. Sikora, N. N. Johannsen, M. E. Allentoft, Unraveling ancestry, kinship, and violence in a Late Neolithic mass grave. *Proc. Natl. Acad. Sci. U.S.A.* **116**, 10705–10710 (2019).

116. S. Walsh, L. Chaitanya, K. Breslin, C. Muralidharan, A. Bronikowska, E. Pospiech, J. Koller, L. Kovatsi, A. Wollstein, W. Branicki, F. Liu, M. Kayser, Global skin colour prediction from DNA. *Hum. Genet.* **136**, 847–863 (2017).

117. L. Chaitanya, K. Breslin, S. Zuñiga, L. Wirken, E. Pośpiech, M. Kukla-Bartoszek, T. Sijen, P. de Knijff, F. Liu, W. Branicki, M. Kayser, S. Walsh, The HIrisPlex-S system for eye, hair and skin colour prediction from DNA: Introduction and forensic developmental validation. *Forensic Sci. Int. Genet.* **35**, 123–135 (2018).